PONTIFICIA UNIVERSIDAD CATÓLICA DE CHILE
ESCUELA DE INGENIERÍA

IMPACTS OF HYDROGEN DEMAND AND CLIMATE POLICY SCENARIOS ON THE CHILEAN INTEGRATED HYDROGEN-ELECTRICITY NETWORK

JAVIER ANDRÉS JORQUERA COPIER

Thesis submitted to the Office of Research and Graduate Studies
in partial fulfillment of the requirements for the degree of
Master of Science in Engineering

Advisor:
ÁLVARO HUGO LORCA GÁLVEZ

Santiago de Chile, June 2022

PONTIFICIA UNIVERSIDAD CATÓLICA DE CHILE
ESCUELA DE INGENIERÍA

IMPACTS OF HYDROGEN DEMAND AND CLIMATE POLICY SCENARIOS ON THE CHILEAN INTEGRATED HYDROGEN-ELECTRICITY NETWORK

JAVIER ANDRÉS JORQUERA COPIER

Members of the Committee:
ÁLVARO HUGO LORCA GÁLVEZ
ENZO ENRIQUE SAUMA SANTIS
STEFAN LORENCZIK
DENIS ALEJANDRO PARRA SANTANDER

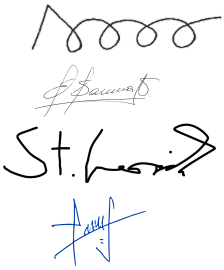

Thesis submitted to the Office of Research and Graduate Studies
in partial fulfillment of the requirements for the degree of
Master of Science in Engineering

Santiago de Chile, June 2022

Gratefully to my parents, brother,
friends, mentors, and colleagues.

ACKNOWLEDGMENTS

ACKNOWLEDGMENTS

This thesis has been by far the most challenging single piece of work I have embarked myself on. I firmly believe that our successes and learnings are not only our own, but also notably of those who have been with us in our journey. Thus, I would like to wholeheartedly thank several people that have supported me in this process and, equally as important, contributed to make me the person I am today.

To my advisor, Álvaro, for his continued support, patience, positive mindset, and all of his understanding through many difficult situations I had to overcome recently. From my university, I thank the other PUC committee members, Enzo, Matías and Denis, and my ECS-Lab colleagues, particularly Lucas and Andrés, for their valuable suggestions and motivation.

To my IEA supervisor, Stefan, for all his teachings and the opportunities he has given me. To Joerg, Mariano and José, for giving me the opportunity to come to the IEA in the first place. To Juha, Anders, Laura G., Manuel, Silvia R., Javier S., Zoe, Pablo H., Alejandra, Emi, Elizabeth, Laura M., Srivatsan, Carlos, Gergely, Peter F., Julia G., Gabriel S., and many other colleagues that I feel incredibly lucky to share a workspace with. I could not have dreamed of a better place than the IEA to begin my formal professional career or better than Paris to continue my life after university.

To my colleagues during my previous internship at the Chilean Ministry of Energy, for giving me an amazing opportunity to start involving myself in discussions and analysis on energy policy and outlooks. Special thanks go Alex, Carlos, Carlos, and Rubén for contributing to this work by remaining available to answer all my questions and hear all the suggestions I had regarding the Ministry's Long Term Planning Process data.

To many mentors I have been supported by in recent years, namely Benjamín Maluenda, Rodrigo Valdés, Javier Boncompte, Loreto Cox, Diego Díaz, Susana Claro and Carlos Álvarez. All your achievements and teachings have motivated me to continue giving my best for the greater good.

To many great friends I have met at the OECD (Luiz H., Ricardo P., Francesco P., Vicky M., Sofía H., Daniela S., and many others) for their continued support, understanding, positive energy, and for sharing great moments with me.

To all the great friends that I made during university times, especially through mentoring, volunteering and student representation work. Thanks a lot Fran, Peñafiel, Jose S., Nathy, Pipe A., Cami R., Richard, Benja A., Gery, Nacho A., Espe, and Gonzalo C.U.. From *Los K*: Nico, JP, Joaco, Jaime, Vicho, Carlos, Diego. From *Oh Canada*: Tisco, Seba, Haase, Barri. The experiences, good and difficult, that I shared with all of you and many other friends, are what I most treasure from these times.

Finally, my biggest thanks go to my relatives. Most importantly, I thank my father, Fernando, my mother, Marcia, and my brother, Eduardo, for their unconditional support and care during all these years, and for pushing me to pursue my dreams despite how far across the ocean they are taking me. I will continue to give my best to honor all the efforts you have made for me.

TABLE OF CONTENTS

LIST OF FIGURES

LIST OF TABLES

ABSTRACT

As countries continue to update their climate ambitions, they are seeking cost-effective solutions for decarbonizing energy use. In this context, low-carbon hydrogen production and use presents relevant opportunities for emission reductions and economic development, and recent studies show important potential benefits from integrating electricity and hydrogen networks. Based on a novel mathematical optimization model, we carry out a case study for Chile in 2020-2050 to assess the least-cost evolution of the integrated hydrogen-electricity system, testing different carbon prices, 100% renewable mandates, and incorporating domestic and international hydrogen demand. By optimizing over various scenarios, we find that, due to the country's significant renewable potential and the flexibility that electrolyzers can provide to the network, adding hydrogen exports to domestic hydrogen use may enhance renewable integration, while not necessarily increasing in electricity prices for typical electricity customers (relative to our baseline), but also make battery deployment less attractive. Further, we conclude that climate policies may be crucial to achieve a fully renewable system by 2050 and reduce cumulative emissions, resulting in 3-14% higher net present system costs. Finally, we discuss that various concerns such as water and land use will have to be addressed by policymakers.

Keywords: Chile, Decarbonization, Integrated energy systems planning, Renewable integration, Hydrogen, Sector coupling.

RESUMEN

A medida que los países actualizan sus ambiciones climáticas, buscan soluciones rentables para descarbonizar el uso energético. En este contexto, la producción y uso de hidrógeno bajo en carbono presenta oportunidades para reducir emisiones y desarrollarse económicamente, y estudios recientes muestran beneficios potenciales de integrar redes de electricidad e hidrógeno. Usando un nuevo modelo de optimización matemática, realizamos un estudio de caso para Chile en 2020-2050 para evaluar la evolución de menor costo del sistema integrado de hidrógeno-electricidad, probando diferentes precios del carbono, mandatos de 100% renovables, e incorporando demanda de hidrógeno nacional e internacional. Optimizando en varios escenarios, encontramos que, dado el importante potencial renovable y a la flexibilidad que los electrolizadores proporcionan al sistema, añadir exportaciones de hidrógeno al consumo doméstico puede aumentar la integración renovable, sin necesariamente aumentar los precios de la electricidad para los clientes típicos (comparado con nuestro caso base), pero también hace que invertir en baterías no sea atractivo. Además, concluimos que las políticas climáticas pueden ser cruciales para lograr un sistema totalmente renovable en 2050 y reducir las emisiones acumuladas, lo que resulta en costos del sistema 3-14% mayores. Por último, discutimos que los responsables políticos deberán considerar diversos aspectos, como el uso de agua y suelo.

Palabras clave: Chile, Descarbonización, Hidrógeno, Integración de renovables, Planificación de sistemas energéticos integrados, *Sector coupling*.

1. INTRODUCTION

1.1. Context

To limit the negative impacts of climate change, 196 countries signed the Paris Agreement in 2015, to keep the global temperature increase well below 2°C in comparison to pre-industrial temperatures (United Nations Framework Convention on Climate Change, n.d.). For that purpose, countries submit Nationally Determined Contributions (NDC), which detail their emissions reduction targets. As of September 2021, most countries had submitted at least their first NDC (IEA, 2021e). Moreover, over 50 countries and the European Union have announced net-zero emissions targets. In 2019, Chile committed to achieving carbon neutrality by 2050 (Prensa Presidencia, 2019).

As energy production and use are responsible for around two-thirds of the global greenhouse gas emissions (IRENA, 2017) and 77% in Chile (Ministerio de Medio Ambiente, 2020), decarbonization plans include measures targeted to abate energy-sector-related emissions. The power sector accounts for around 39% of global energy-related CO_2 emissions (IEA, 2020) and 32% in Chile. Coal-fired generation alone accounts for 28% and 32% of global and Chilean energy-linked CO_2 emissions, respectively. To address this, Chile adopted in 2019 a plan to phase out and/or retrofit all coal-fired power plants at most by 2040 (Ministerio de Energía, 2020c). This can contribute to Chile's ambitions, as reducing power system emissions will be crucial for deep economy-wide decarbonization (IEA, 2021a). However, as the power sector produces under half of the total energy-related emissions, decarbonizing electricity production will need to be complemented with other solutions to achieve climate ambitions cost-effectively.

Hydrogen produced through low-carbon processes (hereafter, low-carbon hydrogen) has gained strong momentum in recent years as an attractive energy vector to support clean energy transitions. Over 35 countries either have published or are currently working on hydrogen strategies (IEA, 2021b). Hydrogen can contribute to deep decarbonization in various hard-to-abate sectors such as mobility and industry (IRENA, 2021a), as its use

as an energy source does not produce direct emissions (IEA, 2019). Thus, its emissions abatement potential rests on the availability of low-carbon means of hydrogen production. In this sense, it can be considered low-carbon hydrogen if it is produced via electrolysis (using water and electricity as inputs) supplied with renewable energy (Vásquez et al., 2019).

By launching its National Green Hydrogen Strategy in November 2020 (Ministerio de Energía, 2020b), Chile became the first Latin American country to publish an official government document setting out ambitions and an action plan for hydrogen deployment. With its goal of having 25 GW of electrolysis capacity built or under development by 2030, it was the first country outside of the European Union with an established electrolysis target (IEA, 2021c). Low-carbon hydrogen is set to play a crucial role in Chile's clean energy transition, as the government expects it to contribute to over 20% of the emissions reductions needed to achieve carbon neutrality by 2050 (Ministerio de Energía, 2020a). Additionally, the hydrogen market is expected to potentially create around 78.000 and 740.000 jobs by 2030 and 2050, respectively, if the ambitions detailed in the Chilean strategy are met (GIZ & HINICIO Chile, 2021).

Chile's hydrogen ambitions for domestic use and exports rely on its large renewable potential, as electricity costs represent 50-90% of hydrogen production costs (IEA, 2021b). Chile has the best solar photovoltaic (PV) resource in the world in some of its northern desert areas, along with the significant potential for other renewables such as onshore wind and hydropower (IEA, 2018). It has been estimated that, from Arica to Chiloé (that is, excluding most of the Chilean Patagonia), Chile potentially has over 1250 GW of solar PV capacity, and around 550 and 40 GW of concentrated solar power (CSP) and wind power, respectively (GIZ & Ministerio de Energía, 2014). This will enable Chile to produce large amounts of low-carbon hydrogen at very competitive costs.

1.2. Integration of power systems with hydrogen networks

Hydrogen can be produced with electricity via electrolysis. Moreover, fuel cells or hydrogen-fired turbines can generate electricity using hydrogen (IEA, 2019). This enables beneficial linkages between both systems. In a recent report by IRENA (2021b), it is stated that connecting the power system with other sectors such as industry or transport, for instance, producing hydrogen that is then employed in vehicles or industrial machinery, could support deeper decarbonization and enable higher variable renewable integration, as is also explained in a recent paper (Stöckl et al., 2021). Moreover, including hydrogen technologies in the energy system could decrease overall system costs (He et al., 2021; vom Scheidt et al., 2022), benefiting from synergies between both systems such as the flexibility of electrolysis, that can take advantage of surplus renewable electricity. To integrate both networks, a wide variety of technologies can be considered, such as power plants, transmission lines, and electric batteries, and also electrolyzers, hydrogen transport via pipelines or trucks, and hydrogen storage. The broad range of technologies and their interactions present important challenges to plan for the best possible integrated system design.

To properly understand the interactions between the hydrogen and electricity networks, allowing to plan for the least-cost integrated network for Chile in the long-term under the effects of various policies, an adequate integrated hydrogen-power system infrastructure planning model is required. There is a vast literature on power systems planning, and Gacitúa et al. (2018) show that optimization-based capacity expansion planning models have been extensively used to study the cost-optimal system evolution under various scenarios. For hydrogen network planning the literature is more recent, and least-cost optimization models are also commonly used (Li et al., 2019; Yang et al., 2020; Samsatli et al., 2016; Bødal et al., 2020; Welder et al., 2018). As for studies that model the integrated network design, the research available tends to focus mostly on one of the networks, including a thorough representation of one system, but simplifying the other (Bødal et al., 2020; Stöckl et al., 2021). Moreover, studies usually focus on one target year for network

design, for example, 2050, such as the paper by Bødal et al. (2020). There is also work that includes a comprehensive representation of the temporal evolution of multi-vector integrated networks, for instance, Samsatli and Samsatli (2018), and without the concurrent study of international hydrogen exports, which is a key part of the Chilean hydrogen ambitions, under a mixed-integer linear optimization framework, or a representation of CSP technologies, of which there is already an operating plant in Chile.

In Chile, there are already some papers analyzing the potential of hydrogen and its potential impacts on the country's energy landscape. However, this work has focused mostly on hydrogen supply (Armijo & Philibert, 2020; Hurtubia & Sauma, 2021; Gallardo et al., 2021). Other recent works (Osorio-Aravena et al., 2021; Osorio Aravena et al., 2020) have analyzed pathways to develop a sustainable Chilean energy system by 2050, modeling the power system connected to sectors such as transport and heat, and considering hydrogen production and use. However, these studies include reduced geographical resolution (six nodes or less for the whole country) and do not consider hydrogen transport or exports. Further, the Ministry of Energy of Chile regularly conducts the Long-term Energy Planning Process to study the optimal power system evolution (Ministerio de Energía, 2021). Even though hydrogen production for domestic and export use is considered, it is only included as an electricity demand source, electrolysis power usage is pre-allocated in a predefined distribution across nodes, and no hydrogen transport or storage is considered. To the best of our knowledge, there is no model purposed to design national-scale hydrogen-power systems, that provides a detailed representation of both networks, their technology diversity and interactions, and enables to assess the system's evolution throughout a long-term horizon under the effects of various climate policies and significant hydrogen exports. Particularly, we are not aware of a Chilean case study that examines these combined developments until 2050. With this work, we address these gaps.

1.3. Objectives and contributions of this work

Given the sketched background, the main objective of this work is to carry out a Chilean case study throughout the 2020-2050 horizon. This is performed with a newly-developed linear optimization model purposed to jointly plan investment and operation of hydrogen and electricity infrastructure, incorporating effects of different climate policies (carbon price, emission limits) and hydrogen demand scenarios (domestic consumption with and without exports), over a long time horizon. The obtained results enable us to assess the implications and the insights they can provide for the policy discussion around hydrogen deployment and integrated system decarbonization.

A summary of the main contributions of this thesis is presented hereafter:

(i) Formulation of an optimization-based linear capacity expansion planning model suited for large-scale integrated hydrogen-electricity systems, adaptable to any country or region. This model allows for allocating hydrogen and electricity production, transport and storage decisions (including seasonal hydrogen storage), hydrogen exports, and the representation of a diverse portfolio of energy technologies and multiple target years, subject to operational and policy constraints.

(ii) The model is employed to carry out a Chilean case study with data already being used for energy policy analysis by the Ministry of Energy of Chile, among other data sources. The results show the most cost-effective investment and operational decisions with temporal and geographical scope, and highlight important synergies between hydrogen and electricity networks.

(iii) Policy assessment of the economic and environmental implications that can be derived from the results of the case study. This includes the effects of domestic hydrogen demand, hydrogen exports, carbon pricing, and 100% renewable mandates over the most cost-effective investment portfolio, electricity and hydrogen supply prices, emissions, system costs, and the system's operation.

The remainder of this thesis is organized as follows. Chapter 2 describes the methodology used. Chapter 3 presents the characteristics and key assumptions of the case study that was carried out. In Chapter 4 we present and discuss the obtained results. Lastly, in Chapter 5 we draw conclusions, policy implications, and discuss directions for further research.

2. METHODOLOGY

2.1. Proposed integrated hydrogen-electricity network planning model

We developed a mathematical optimization model to plan for the least-cost integrated energy system at energy production and transport level (that is, without accounting for other investments such as distribution networks). The model ensures that demand for both hydrogen and electricity is met at all times and in all locations at minimum cost, incorporating system operation and investment constraints under a linear optimization framework. The integrated system is modeled as two parallel (hydrogen and electricity) networks (see Figure 2.1). Each node can have supply and storage units, energy inflows and outflows, and energy vector demand. The coupling of the two systems is enabled by the possibility to produce hydrogen using electricity or vice versa.

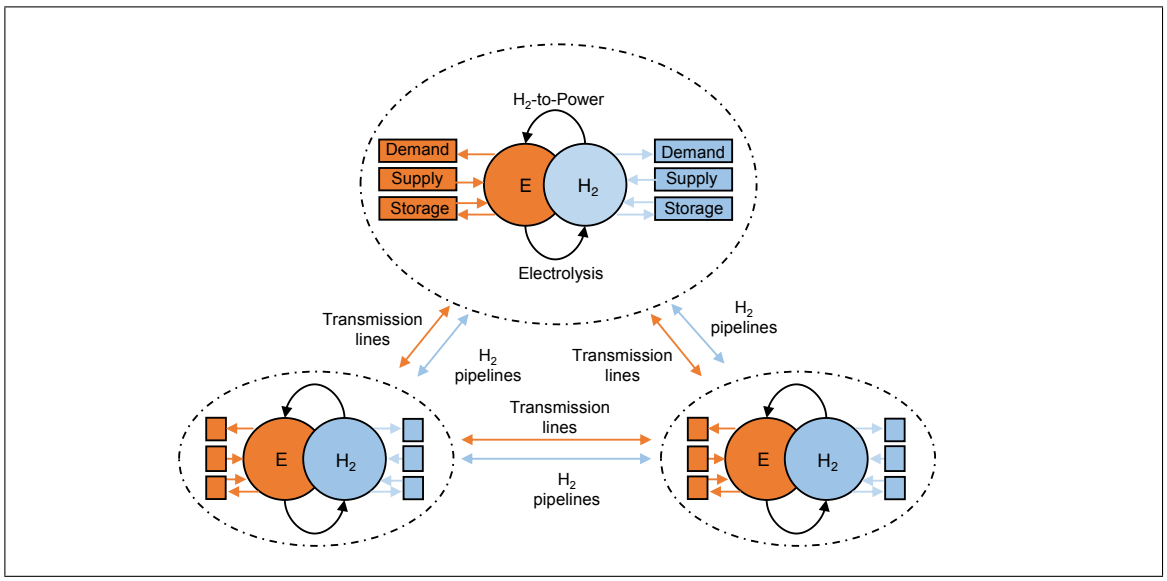

Figure 2.1. Diagram of the integrated hydrogen-electricity system.

Throughout the planning horizon, investment and operational decisions are modeled only for a set $\mathcal{Y}$ of target years. On an operational level, a set of representative days is used to model the operational dynamics throughout every target year, in line with existing

literature on capacity expansion planning models for energy policy analysis (Gacitúa et al., 2018). This approach enables the model to provide a reasonable representation of the daily operational requirements to be met by the system, safeguarding computational tractability.

The mathematical representation is presented below (Eqs. 2.1a - 2.7), with variables in capital letters and model inputs in lower case letters. The comprehensive nomenclature is available in Appendix A.

2.1.1. Objective function

Eqs. (2.1a) - (2.1f) break down the objective function, which minimizes the net present value (NPV) of the total costs throughout the planning horizon. The total cost C_y^T for every target year y is split into investment, fixed, and variable operational costs. The investment costs consider the annualized cost of investments made in every target year y, taking into account that if the investment cost of capacity addition $B_{unit,y'}$ was different in year y', then the annualized cost paid in year y must reflect the cost at the moment of deployment. This enables the model to correctly capture the investment dynamics under steep learning curves. The fixed costs include non-variable annual operation and maintenance costs of the deployed units. The variable operational costs embrace expenses such as the direct cost of energy production and estimated CO_2 tax costs. To estimate the total costs $C_{y+y^I}^{T'}$ for every intermediate year $y + y^I$, a linear approximation is used, based on the constant period k between consecutive target years, and the set $\mathcal{Y}^I = \{0, .., k-1\}$.

$$\min \quad \sum_{y \in \mathcal{Y} - \mathcal{Y}_{end}} \sum_{y^I \in \mathcal{Y}^I} d^{factor}_{y+y^I} C^{T'}_{y+y^I} + d^{factor}_{\mathcal{Y}_{end}} C^{T}_{\mathcal{Y}_{end}} \tag{2.1a}$$

$$\text{s.t.} \quad C^{T'}_{y+y^I} = C^T_y + (C^T_{y+k} - C^T_y)\frac{y^I}{k} \qquad \forall y \in \mathcal{Y} - \mathcal{Y}_{end}, y^i \in \mathcal{Y}^i \tag{2.1b}$$

$$C^T_y = InvCosts_y + FixedCosts_y + OpCosts_y \qquad \forall y \in \mathcal{Y} \tag{2.1c}$$

$$InvCosts_y = \sum_{y' \leq y} (\sum_{g \in \mathcal{G}} c^{G,inv}_{gy'} B^G_{gy'} + \sum_{g \in \mathcal{G}^{ES}} c^{ES,inv}_{gy'} B^{ES}_{gy'} + \sum_{l \in \mathcal{L}} c^{L,inv}_{ly'} B^L_{ly'}) \qquad \forall y, y' \in \mathcal{Y} \tag{2.1d}$$

$$FixedCosts_y = \sum_{g \in \mathcal{G}} c^{G,fix}_{gy} K^G_{gy} + \sum_{g \in \mathcal{G}^{ES}} c^{ES,fix}_{es,y} K^G_{gy} + \sum_{l \in \mathcal{L}} c^{L,fix}_{ly} K^L_{ly} \qquad \forall y \in \mathcal{Y} \tag{2.1e}$$

$$VarOpCosts_y = \sum_{t \in \mathcal{T}} \omega_t \sum_{g \in \mathcal{G}} (c^{vom}_g + h_g c^{fuel}_{gy} + \eta^{CO_2}_g c^{CO_2 tax}_y) P_{gty} \qquad \forall y \in \mathcal{Y} \tag{2.1f}$$

2.1.2. Energy balance and transport constraints

The energy balance constraints (2.2a) - (2.2f) ensure that, for each node n, the sum of the energy inflows and outflows is equal at all times. The variable $D^{H_2}_{E,nty}$ is included in the power balance (2.2a) to freely allocate electrolysis power consumption. Similarly, the hydrogen balance constraint (2.2b) models the fuel demand of hydrogen-based generators ($D^E_{H_2,nty}$). Energy vector consumption of electrolyzers and hydrogen-to-power units is defined by Eqs. (2.2c) - (2.2d) respectively. Further, Eq. (2.2e) ensures that enough hydrogen is delivered to a subset of export nodes to meet the export demand every year y, allocating it freely across those nodes. Finally, energy transport flows are governed by a simple linear model (2.2f).

$$\sum_{g\in\mathcal{G}_n^E} P_{gty}^E + \sum_{l\in\mathcal{L}_n^{E,in}} \eta_l^{E,L} F_{lty}^E = d_{nty}^{E,base} \tag{2.2a}$$
$$+ D_{E,nty}^{H_2} + \sum_{l\in\mathcal{L}_n^{E,out}} F_{lty}^E + \sum_{g\in\mathcal{G}_n^{BES}} Q_{gty}^{E,C} \qquad \forall n\in\mathcal{N}, t\in\mathcal{T}, y\in\mathcal{Y}$$

$$\sum_{g\in\mathcal{G}_n^{H_2}} P_{gty}^{H_2} + \sum_{l\in\mathcal{L}_n^{H_2,in}} \eta_l^{H_2,L} F_{lty}^{H_2} = d_{nty}^{H_2,base} + D_{H_2,nty}^E \tag{2.2b}$$
$$+ D_{nty}^{H_2,export} + \sum_{l\in\mathcal{L}_n^{H_2,out}} F_{lty}^{H_2} + \sum_{g\in\mathcal{G}_n^{HES}} Q_{gty}^{H_2,C} \qquad \forall n\in\mathcal{N}, t\in\mathcal{T}, y\in\mathcal{Y}$$

$$D_{E,nty}^{H_2} = \sum_{g\in\mathcal{G}_n^{H_2}} (\lambda_y^{H_2,prod} + \lambda^{H_2,comp}) P_{gty} \qquad \forall n\in\mathcal{N}, t\in\mathcal{T}, y\in\mathcal{Y} \tag{2.2c}$$

$$D_{H_2,nty}^E = \sum_{g\in\mathcal{G}_n^{H_2toP}} \lambda_g^{H_2toP} P_{gty} \qquad \forall n\in\mathcal{N}, t\in\mathcal{T}, y\in\mathcal{Y} \tag{2.2d}$$

$$\sum_{n\in\mathcal{N}^{export}} D_{H_2,nty}^{export} \geq d_{H_2,y}^{export} \qquad \forall y\in\mathcal{Y} \tag{2.2e}$$

$$-K_{ly}^L \leq F_{lbt} \leq K_{ly}^L \qquad \forall\, l\in\mathcal{L}, t\in\mathcal{T}, y\in\mathcal{Y} \tag{2.2f}$$

2.1.3. Supply constraints

Eqs. (2.3a) and (2.3b) respectively limit energy vector production for non-variable and variable assets, considering availability and time-variant capacity factors. Additionally, based on work by Mena et al. (2019), Eqs. (2.3c)-(2.3g) thoroughly represent the dynamics of CSP units. The non-linearities depicted by the equations only involve parameters, therefore preserving the linearity of the model. Eqs. (2.3c), (2.3d) and (2.3e) respectively model the thermal power balance, charging, and discharging limits, whereas (2.3f) governs the thermal energy storage limit. Lastly, Eq. (2.3g) sets the cyclic thermal energy balance of each unit.

$$0 \leq P_{gty} \leq \eta_g K^G_{gy} \qquad \forall g \in \mathcal{G} - \mathcal{G}^{PV,wind\&hydro}, t \in \mathcal{T}, y \in \mathcal{Y} \tag{2.3a}$$

$$0 \leq P_{gty} \leq \eta_g \eta_{gt} K^G_{gy} \qquad \forall g \in \mathcal{G}^{PV,wind\&hydro}, t \in \mathcal{T}, y \in \mathcal{Y} \tag{2.3b}$$

$$q^{\mathrm{SF}}_{gt} \geq \frac{P_{gty}}{\eta_g^{\mathrm{SF/TES-PB}} \eta_g^{\mathrm{PB}}} + \frac{Q^{\mathrm{C}}_{gty}}{\eta_g^{\mathrm{SF-TES}}} - \eta_g^{\mathrm{TES-PB}} Q^{\mathrm{D}}_{gty} \qquad \forall g \in \mathcal{G}^{\mathrm{CSP}}, t \in \mathcal{T}, y \in \mathcal{Y} \tag{2.3c}$$

$$0 \leq Q^{\mathrm{C}}_{gty} \leq Q^{\mathrm{SF}}_{gt} \qquad \forall g \in \mathcal{G}^{\mathrm{CSP}}, t \in \mathcal{T}, y \in \mathcal{Y} \tag{2.3d}$$

$$0 \leq \eta_g^{\mathrm{TES-PB}} Q^{\mathrm{D}}_{gty} \leq \frac{P_{gty}}{\left(\eta_g^{\mathrm{SF/TES-PB}} \eta_g^{\mathrm{PB}}\right)} \qquad \forall g \in \mathcal{G}^{\mathrm{CSP}}, t \in \mathcal{T}, y \in \mathcal{Y} \tag{2.3e}$$

$$0 \leq E^{\mathrm{TES}}_{gty} \leq \frac{K^{\mathrm{G}}_{gy}}{\eta_g^{\mathrm{PB}} \eta_g^{\mathrm{SF/TES-PB}} \eta_g^{\mathrm{TES-PB}}} \Delta t_g^{\mathrm{TES}} \qquad \forall g \in \mathcal{G}^{\mathrm{CSP}}, t \in \mathcal{T}, y \in \mathcal{Y} \tag{2.3f}$$

$$E^{\mathrm{TES}}_{gty} = \eta_g^{\mathrm{TES}} E^{\mathrm{TES}}_{g,t-1,y} + \Delta_{t,t-1} \left(Q^{\mathrm{C}}_{g,t-1,y} - Q^{\mathrm{D}}_{g,t-1,y}\right) \qquad \forall g \in \mathcal{G}^{\mathrm{CSP}}, t \in \mathcal{D}_r, \mathcal{D}_r \in \mathcal{D}, y \in \mathcal{Y} \tag{2.3g}$$

2.1.4. Storage constraints

Eqs. (2.4a) - (2.4h) govern the operational and investment dynamics for the set $\mathcal{G}^{ES}$ of all storage units, inspired by the work by Verástegui et al. (2020). The non-linearities depicted by the equations only involve parameters, therefore preserving the linearity of the model. The storage representation used represents intra-daily decisions for all technologies, with additional flexibility for seasonal storage in the case of hydrogen only. Eq. (2.4a) defines the total inverter (or compressor) capacity available every year y, whereas

Eq. (2.4b) defines the hydrogen storage capacity. Investments in battery storage are directly linked to inverter capacity via the parameter γ_g, which indicates the hours of storage of battery g (2.4e). Further, investments in compressor (B_g^{ES}) and hydrogen storage capacity ($B_g^{H_2S}$) are done independently. Eq. (2.4c) defines the charging limits and (2.4d) defines the intra-day cyclic energy balance for batteries. To model the seasonal storage of hydrogen, we adapted the linked representative days method described by Gonzato et al. (2021). Eq. (2.4f) defines the cyclic hydrogen balance constraint, connecting consecutive representative days and ensuring that the last time segment of the year is linked to the first. Eq. (2.4g) defines a second cycling constraint to ensure non-negative annual net discharges. Eq. (2.4h) sets the hydrogen inventory limit based on its installed capacity.

$$K_{gy}^{G} = \sum_{y' \leq y} B_{gy'}^{G} \qquad \forall g \in \mathcal{G}^{\mathrm{ES}}, y, y' \in \mathcal{Y} \tag{2.4a}$$

$$K_{gy}^{ES} = \sum_{y' \leq y} B_{gy'}^{ES} \qquad \forall g \in \mathcal{G}^{\mathrm{H_2S}}, y, y' \in \mathcal{Y} \tag{2.4b}$$

$$Q_{gty}^{C} \leq K_{gy}^{ES} \eta_g^{ES} \qquad \forall g \in \mathcal{G}^{\mathrm{ES}}, t \in \mathcal{T}, y \in \mathcal{Y} \tag{2.4c}$$

$$E_{gty}^{ES} = E_{g,t-1,y}^{B} + \Delta_{t,t-1}(\sqrt{\eta_g^{ES}} Q_{g,t-1,y}^{C} - \frac{P_{g,t-1,y}}{\sqrt{\eta_g^{ES}}}) \qquad \forall g \in \mathcal{G}^{\mathrm{BES}}, t \in \mathcal{D}_r, \mathcal{D}_r \in \mathcal{D}, y \in \mathcal{Y} \tag{2.4d}$$

$$0 \leq E_{gty}^{ES} \leq \gamma_g K_{gy}^{G} \qquad \forall g \in \mathcal{G}^{\mathrm{ES}}, t \in \mathcal{T}, y \in \mathcal{Y} \tag{2.4e}$$

$$E_{gty}^{ES} = E_{g,t-1,y}^{B} + \Delta_{t,t-1}(\sqrt{\eta_g^{ES}} Q_{g,t-1,y}^{C} - \frac{P_{g,t-1,y}}{\sqrt{\eta_g^{ES}}}) \qquad \forall g \in \mathcal{G}^{\mathrm{H_2S}}, t \in \mathcal{T}, y \in \mathcal{Y} \tag{2.4f}$$

$$0 \leq \sum_{t \in \mathcal{T}} \omega_t (Q_{gty} - P_{gty}) \qquad \forall g \in \mathcal{G}^{H_2S}, y \in \mathcal{Y} \tag{2.4g}$$

$$0 \leq E_{gty}^{ES} \leq K_{gy}^{ES} \qquad \forall g \in \mathcal{G}^{\mathrm{H_2S}}, t \in \mathcal{T}, y \in \mathcal{Y} \tag{2.4h}$$

2.1.5. Investment and availability constraints

To properly represent the capacity expansion, Eqs. (2.5a) - (2.5h) set asset investment and availability constraints for all technologies. The units are separated into three categories: existing, planned, and candidates. For existing and planned units, their available capacity $K_{unit,y}$ depends both on its nominal capacity and a binary input parameter $\delta_{unit,y}$ that is defined to account for phase-ins or phase-outs. For the candidate units, non-negative, continuous investment decisions can be made in each period for every unit, meaning that the capacity installed in one year can be later increased. The cumulative installed capacity for each candidate asset every period is the sum of all investments on it up to that year. The maximum available capacity of every candidate unit is limited both by its earliest possible year of entry to the system and by a unit-specific capacity cap.

$$K^G_{gy} = \delta_{gy} p^{max}_g \qquad \forall g \in \mathcal{G}_{ex} \cup \mathcal{G}_{plan}, y \in \mathcal{Y} \tag{2.5a}$$

$$K^G_{gy} = \sum_{y' \leq y} B^G_{g,y'} \qquad \forall g \in \mathcal{G}_{cand}, y \in \mathcal{Y} \tag{2.5b}$$

$$K^L_{ly} = \delta_{ly} f^{max}_l \qquad \forall l \in \mathcal{L}_{ex} \cup \mathcal{L}_{plan}, y \in \mathcal{Y} \tag{2.5c}$$

$$K^L_{ly} = \sum_{y' \leq y} B^L_{l,y'} \qquad \forall l \in \mathcal{L}_{cand}, y \in \mathcal{Y} \tag{2.5d}$$

$$K^G_{gy} \leq \delta_{gy} \overline{k^G_g} \qquad \forall g \in \mathcal{G}_{cand}, y \in \mathcal{Y} \tag{2.5e}$$

$$K^L_{ly} \leq \delta_{ly} \overline{k^L_l} \qquad \forall l \in \mathcal{L}_{cand}, y \in \mathcal{Y} \tag{2.5f}$$

$$0 \leq B^L_{ly} \qquad \forall l \in \mathcal{L}, y \in \mathcal{Y} \tag{2.5g}$$

$$0 \leq B^G_{gy} \qquad \forall g \in \mathcal{G}, y \in \mathcal{Y} \tag{2.5h}$$

2.1.6. Electricity reliability constraints

Electricity reliability constraints (2.7a) - (2.7c) are included in the model to safeguard system operation while enabling higher variable renewable energy integration. Based on

the work by Quiroga et al. (2019), a set $\mathcal{G}^E_{disp}$ of dispatchable power sources is defined, including fossil-fueled, CSP, hydro dam, electric battery, and hydrogen-fueled units. In each time segment t, the remnant dispatchable power output capacity must be greater or equal to a share of the variable renewable generation plus a share of the current electricity demand. This modeling scheme supports higher reliability via increased available dispatchable capacity, to address short-term variations in variable renewable generation. This allows for higher integration of these technologies without overly risking system reliability. We include reserve constraints to a system's extent, but also to a geographical-zones-based extent, to ensure reliability and security of supply through various geographical scopes of the network.

Moreover, Eq. (2.7c) defines a simplified systemic inertia requirement. Here, in^Y_y corresponds to the system inertia demand, constant within each year. Finally, in^G_g is a scaled inertia factor, equivalent to the ratio of maximum inertia contribution and maximum generation capacity of each unit.

$$\sum_{g\in\mathcal{G}^E_{disp}}(K_{gy}-P_{gty}) \geq \gamma_1 \sum_{g\in\mathcal{G}^{VRE}} P_{gty} + \gamma_2 \sum_{n\in\mathcal{N}}(d^{base}_{nty}+D^{H_2}_{elec,nty}) \qquad \forall t\in\mathcal{T}, y\in\mathcal{Y} \tag{2.6a}$$

$$\sum_{g\in\mathcal{G}^E_{disp}\cap G_z}(K_{gy}-P_{gty}) \geq \gamma_1 \sum_{g\in\mathcal{G}_{VRE}\cap G_z} P_{gty} + \gamma_2 \sum_{n\in\mathcal{N}_z}(d^{base}_{nty}+D^{H_2}_{elec,nty}) \qquad \forall z\in\mathcal{Z}, t\in\mathcal{T}, y\in\mathcal{Y} \tag{2.6b}$$

$$\sum_{g\in G^E} in^G_g P_{gty} \geq in^Y_y \qquad \forall t\in\mathcal{T}, y\in\mathcal{Y} \tag{2.6c}$$

2.1.7. Emissions limit

Finally, besides modeling CO_2 tax costs in the objective function, we include an emissions limit constraint (2.7). It ensures that annual systemic CO_2 emissions of non-renewable generators in each target year y do not exceed a specific emissions cap. This allows for studying various emissions limit trajectories, such as a 100% renewable mandate by the end of the planning horizon or starting from an earlier year. This constraint can be dropped out or a large enough cap can be set if no emissions limit is desired.

$$\sum_{g \in \mathcal{G}^{NonRE},\, t \in \mathcal{T}} \eta_g^{CO_2} h_t P_{gty} \leq cap_y \qquad \forall y \in \mathcal{Y} \tag{2.7}$$

3. CASE STUDY

We carried out a 2020-2050 Chilean energy system case study. To this end, we defined several aspects of the case study in terms of electricity and hydrogen network representation, energy demand, and scenarios, which are described below. A compilation of some key characteristics of this exercise is available in Table 3.1.

Table 3.1. Summary of the case study characteristics.

Time Horizon	Target years	Nodes	Transport corridors	Power Plants	RD's	Time segments per RD
2020-2050	2020, 2030, 2040, 2050	26	28	1172	12	9

Note: RD = representative day.

Source: Adapted from Ministerio de Energía (2020d).

3.1. Power system representation

For the power system definition, we use data from the 2020 *Proceso de Planificación Energética de Largo Plazo* (Long-term Energy Planning Process), led by the Ministerio de Energía (2020d). The data set includes an aggregated representation of the national power system called *Sistema Eléctrico Nacional* (SEN), which runs from the northern area of Chile to the island of Chiloé (see Figure 3.4). Tables C.1 and C.2 present the nodal number-name equivalence and the zonal grouping used, respectively. The database hosts a portfolio of over a thousand power generation units including existing, planned, and candidate assets, with detail on their techno-economic parameters (for example, we present the CAPEX cost projections used in Figures 3.1 and 3.2) and on planned phase-outs (such as the coal power phase-out target committed for no later than 2040). Figure 3.3 shows the projected average generation costs for fossil-fueled plants. Tables C.3 and C.4 illustrate the number of existing generators and planned and candidate units per zone, respectively. We used scenario E of the database, as it is the scenario that was created considering future hydrogen deployment. Individual lines were aggregated to transport corridors, and there

was no capacity limit set for candidate lines. Generation technologies modeled include fossil-fueled, solar PV, wind, CSP (11 and 14 hours of storage), and hydroelectric plants, among others such as electric batteries. The temporal generation profiles for hydro-power were based on 2020's operation results of the Ministry's process. Additionally, based on a recent study by Lorca et al. (2020), a 20% reduction in water resource availability throughout 2020-2050 was considered. We added one hydrogen combined-cycle gas turbine (H_2CCGT) plant and one electric battery as candidate units in every node, without setting a maximum capacity addition. H_2CCGT plants were the technology selected for hydrogen-to-power generation (assumptions presented in Table 3.2), as they were found to be the most cost-effective hydrogen reconversion pathway in a recent study (Welder et al., 2019). Their inertia contribution factor was defined based on the average factor of the natural gas-fired plants. Finally, we defined that candidate assets can only be installed after 2020.

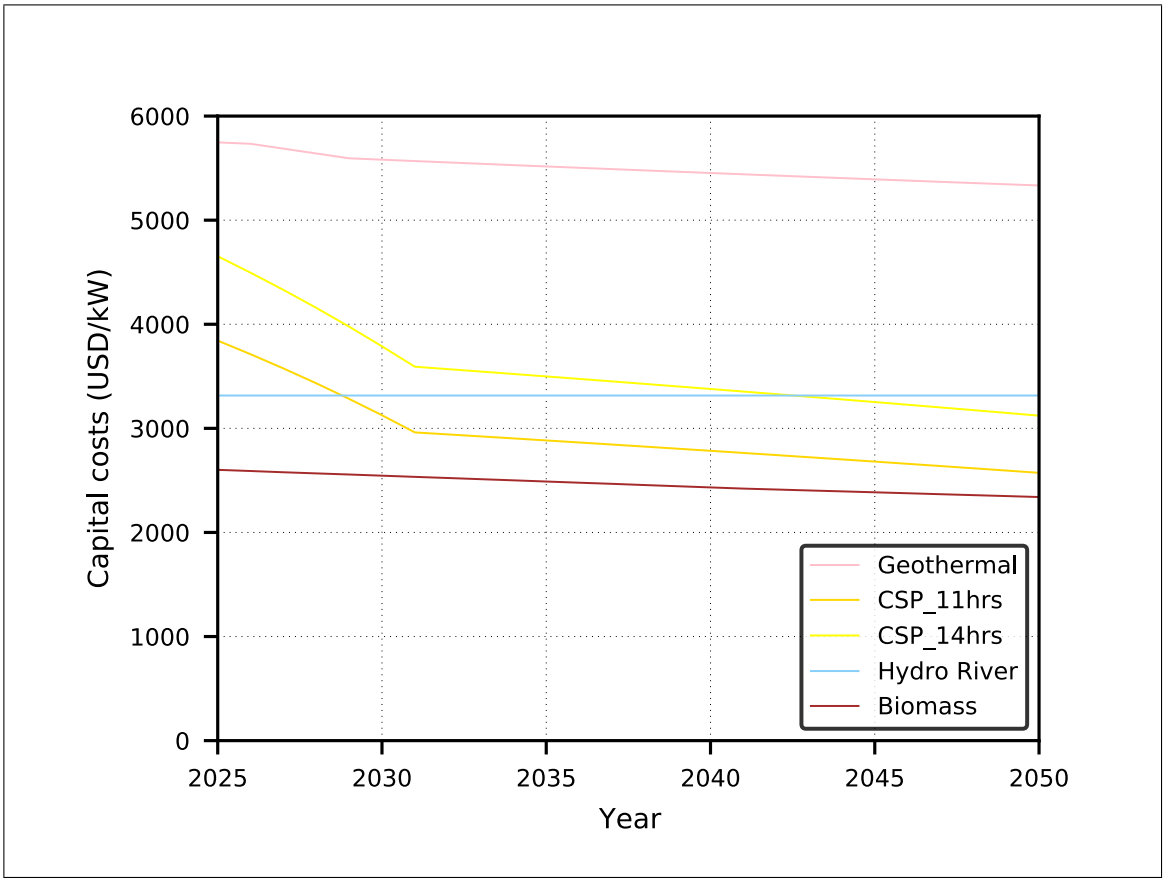

Figure 3.1. CAPEX costs evolution (part 1).
Source: Own elaboration based on Ministerio de Energía (2020d).

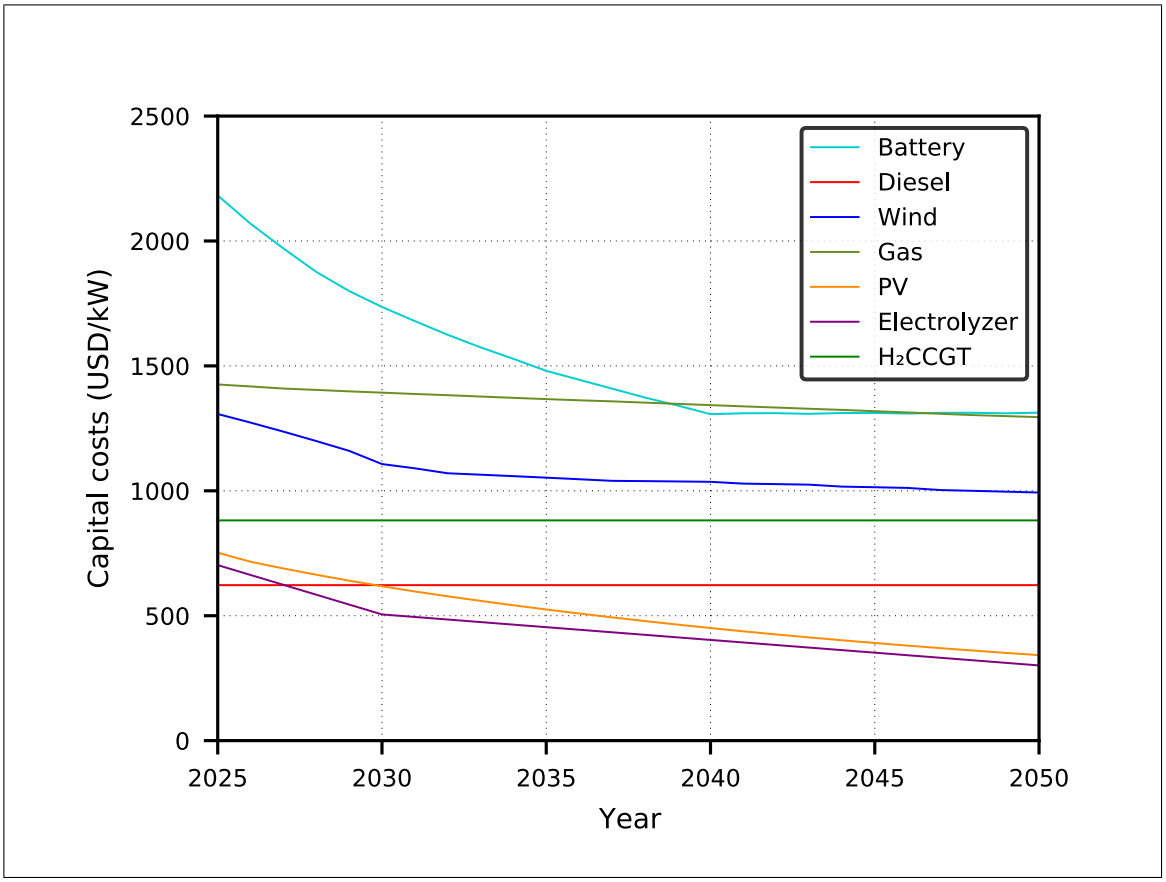

Figure 3.2. CAPEX costs evolution (part 2).
Source: Own elaboration based on Ministerio de Energía (2020d), IEA (2021b), all rights reserved, and Welder et al. (2019).

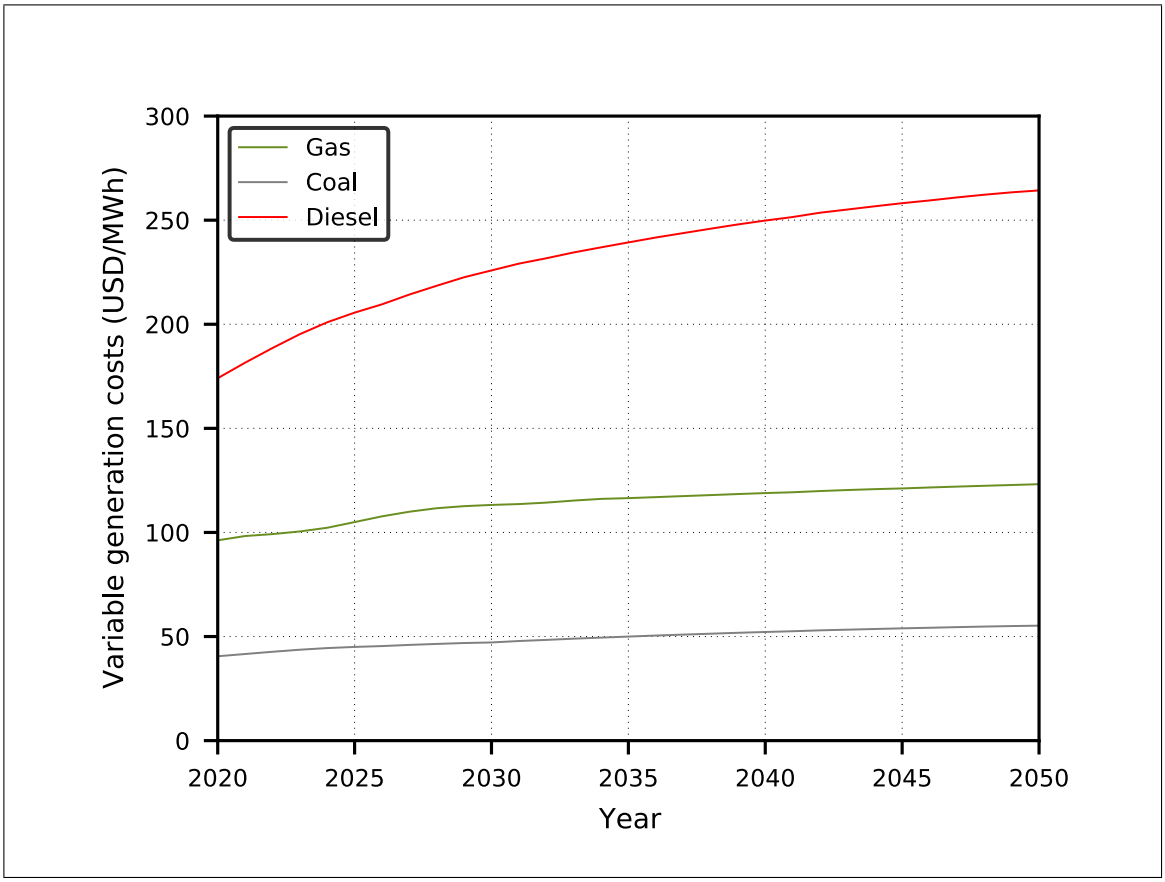

Figure 3.3. Fossil-fuel-based electricity generation variable cost projections (including fuel and variable operation and maintenance costs).
Source: Own elaboration based on Ministerio de Energía (2020d).

Table 3.2. Hydrogen CCGT parameters.

Parameter	Unit	Value
Capital cost	USD/kW	851.2
Non-combustible variable operational costs	USD/MWh$_{el}$	2.6432
Fixed costs	USD/(MW$_{el}$· year)	12405.12
Lifetime	years	25

Source: Welder et al. (2019)

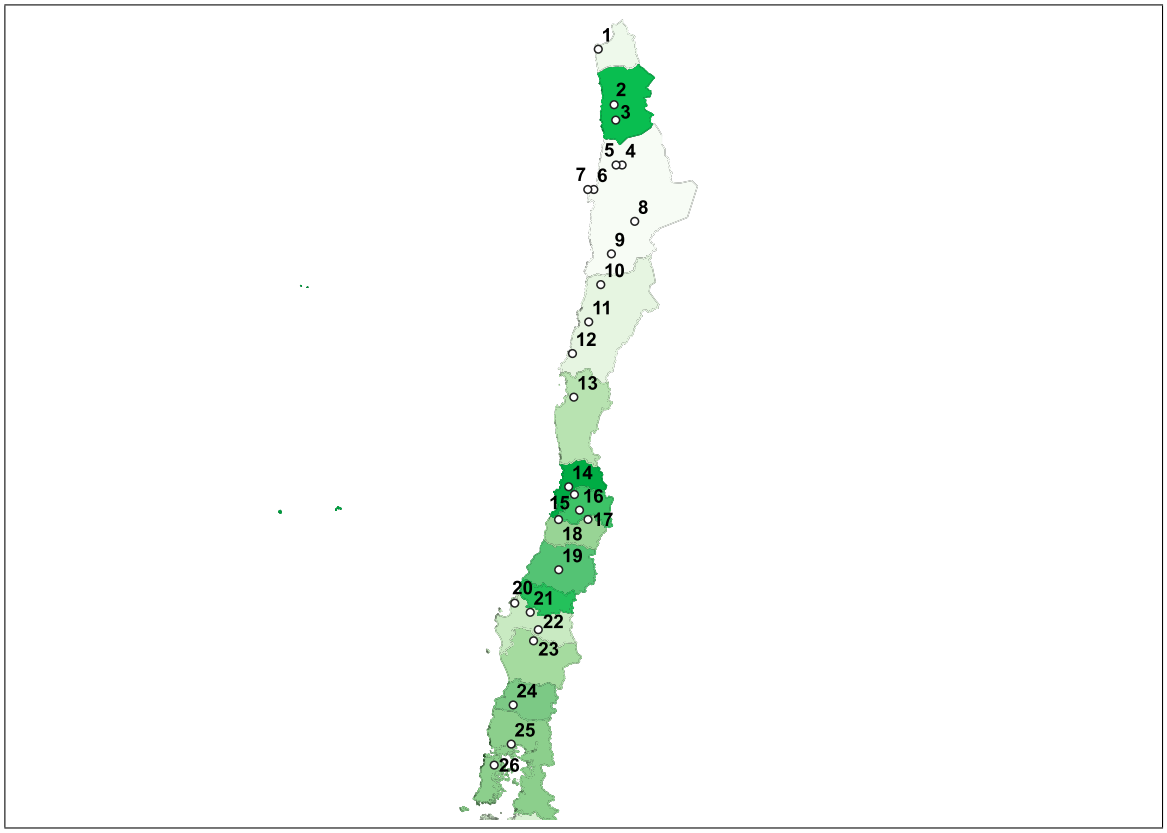

Figure 3.4. Geographical distribution of the nodes of the representation used for the Chilean energy system.
Source: Own elaboration based on Ministerio de Energía (2020d).

3.2. Hydrogen network representation

The hydrogen network was set to mimic the power system's topology, resulting in no energy demand, supply, or flows being considered beyond the Bío Bío region (i.e. beyond node 26). For hydrogen production, only electrolyzers are included (Table 3.3), as they are the only hydrogen supply technology for which Chile set deployment targets (Ministerio de Energía, 2020b). For storage, hydrogen tanks were considered (Table 3.4). For hydrogen transport, we modeled newly-built hydrogen pipelines, as pipelines are the best-suited technology for large volumes of hydrogen transport over long distances (Reuß et al., 2017). No cap was set for capacity additions of electrolyzers, hydrogen storage

or pipelines. Three hydrogen export nodes (6, 15, and 20) were defined based on their proximity to existing ports (Mejillones, Valparaíso, and Talcahuano, respectively).

Table 3.3. Electrolyzer parameters.

Parameter	Unit	Value
Capital cost (in 2020)	USD/kW_{el}	1375
Capital cost (in 2030)	USD/kW_{el}	420
Capital cost (in 2050)	USD/kW_{el}	330
Efficiency (in 2020)	%	64
Efficiency (in 2030)	%	69
Efficiency (in 2050)	%	74
Stack replacement cost (at half of lifetime)	% of CAPEX	35
O&M costs	% of CAPEX (annual)	2.25
Lifetime	years	30

Sources: IEA (2021b), all rights reserved; Agora Energiewende and AFRY Management Consulting (2021).

Table 3.4. Hydrogen storage parameters.

Parameter	Unit	Value
Compression capital cost	USD/(kg/h)	1540
Storage capital cost	USD/kg	516
Compression O&M costs	USD/(kg/h) (annual)	46
Storage O&M costs	USD/kg (annual)	2
Compression power consumption	kWh/kg	1.284
Round-trip efficiency	%	100%
Lifetime	years	40

Source: Bødal et al. (2020).

Table 3.5. Hydrogen pipeline parameters.

Parameter	Unit	Value
Capital cost (reference case)	MUSD/(GW$_{H_2}$ · km)	0.6
Capital cost (high case)	MUSD/(GW$_{H_2}$ · km)	1.484
O&M costs	% of CAPEX (annual)	1.25
Lifetime	years	30

Source: Jens, Wang, van der Leun, Peters, and Buseman (2021).

Note: The capital costs reported include pipeline and compressor costs.

3.3. Energy demand forecasts

The electricity and domestic hydrogen demand forecasts were also sourced from scenario E of the Ministry's database (Ministerio de Energía, 2020d). The operational aspects of the data set are based on 12 representative days, with 9 length-varying time segments each, that represent the energy system's annual operation. Hydrogen demand every year is split equally into every hour, in line with Bødal et al. (2020). The estimated domestic annual hydrogen demand used in this study, illustrated in Figure 3.5, reaches 1160 kton (almost 39 TWh$_{H_2}$) of hydrogen per year by 2050, around 1.2% of global hydrogen demand in 2020 (IEA, 2021b). The domestic hydrogen demand forecast, available in the Ministry's database, considers the following end uses: fuel cell trucks in freight transport, replacement of diesel engines in industry and mining, and replacement of residential and industrial natural gas. The regions with the largest expected domestic demand by 2050 are the second (nodes 5 to 9) and thirteenth regions (nodes 15 and 16), with respective shares of around 27% and 23%, compared with the national total. Figure 3.6 shows the base demand for electricity and hydrogen per node in 2050. Additional export demand, which would amount to 3100 extra ktonH$_2$ (about 103 TWh$_{H_2}$), was estimated based on the Chilean strategy (Ministerio de Energía, 2020b), derived from the ratio of the forecast market size of the hydrogen exports trade versus the domestic use.

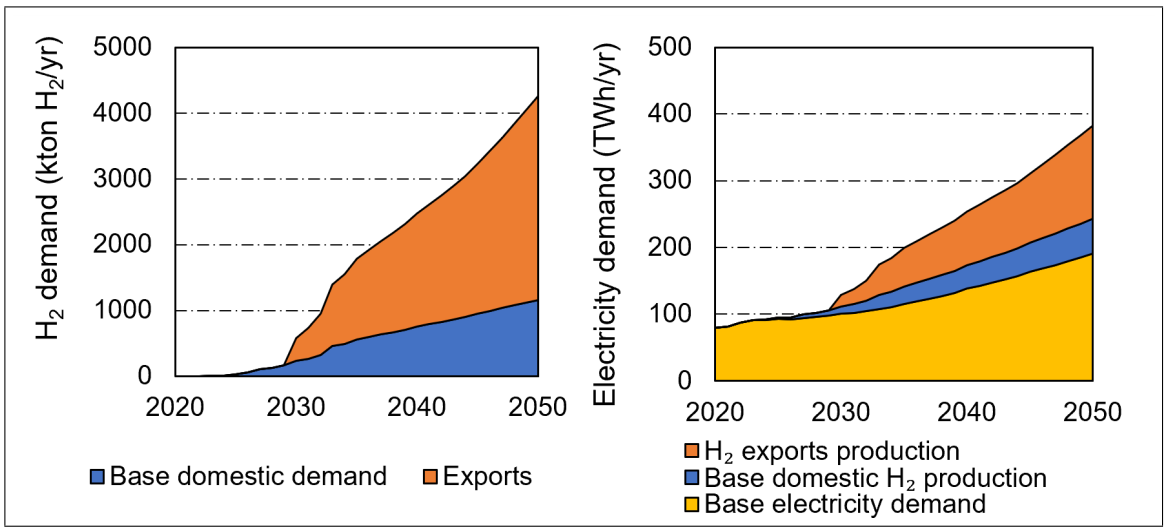

Figure 3.5. Electricity and hydrogen demand forecasts used in this study. **Source:** Own elaboration based on Ministerio de Energía (2020d) and Ministerio de Energía (2020b).
Note: The electrolysis electricity usage was derived from the hydrogen demand forecast and the electrolyzer efficiency projection, assuming a lower heating value of 33.3 kWh/kgH_2. Potential extra hydrogen demand for H_2CCGT plants is not included, as it a case study outcome.

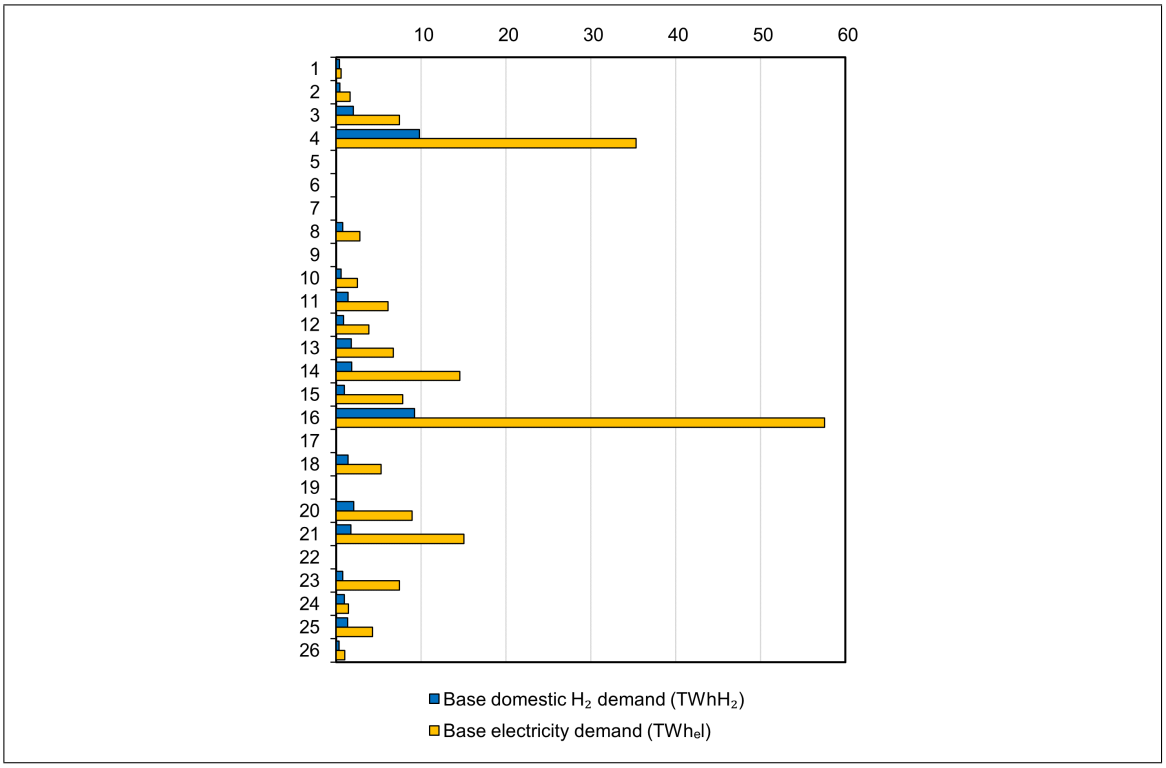

Figure 3.6. Nodal distribution of energy vector demand, 2050.
Source: Own elaboration based on Ministerio de Energía (2020d).

3.4. Scenarios analyzed

To assess the cost-optimal system development under various policy frameworks and two different hydrogen demand levels, several scenarios were developed, based on the projected carbon tax, the year of the 100% renewable ambition for the system (if any), and the addition of hydrogen exports demand. For the 100% renewable scenarios, reaching that goal implies phasing out all non-renewable capacity in the defined year. The Baseline scenario assumes that the current carbon tax of 5 USD/tCO_2 does not change until 2050, there is no renewable mandate or hydrogen exports. BHT serves as a comparison to the Baseline scenario to assess the impact of imposing higher carbon pricing, based on a carbon tax trajectory proposed in a recent IEA study (IEA, 2021d). Figure 3.7 showcases both

carbon price trajectories studied. The 100% renewable by 2050 scenario (RE2050) simulates the current Chilean carbon neutrality pledge, maintaining the current carbon price. Further, we study a 100% renewable by 2040 scenario, to assess the effects of advancing that goal by 10 years. Finally, we developed three hydrogen exports scenarios. H_2EXP adds hydrogen export demand to the baseline scenario to study the effects of significant extra hydrogen demand. Over H_2EXP, we introduce H_2EXPHT and H_2EXPHPC to study the effects of a higher tax and higher pipeline costs, respectively. Table 3.6 summarizes all the scenarios studied.

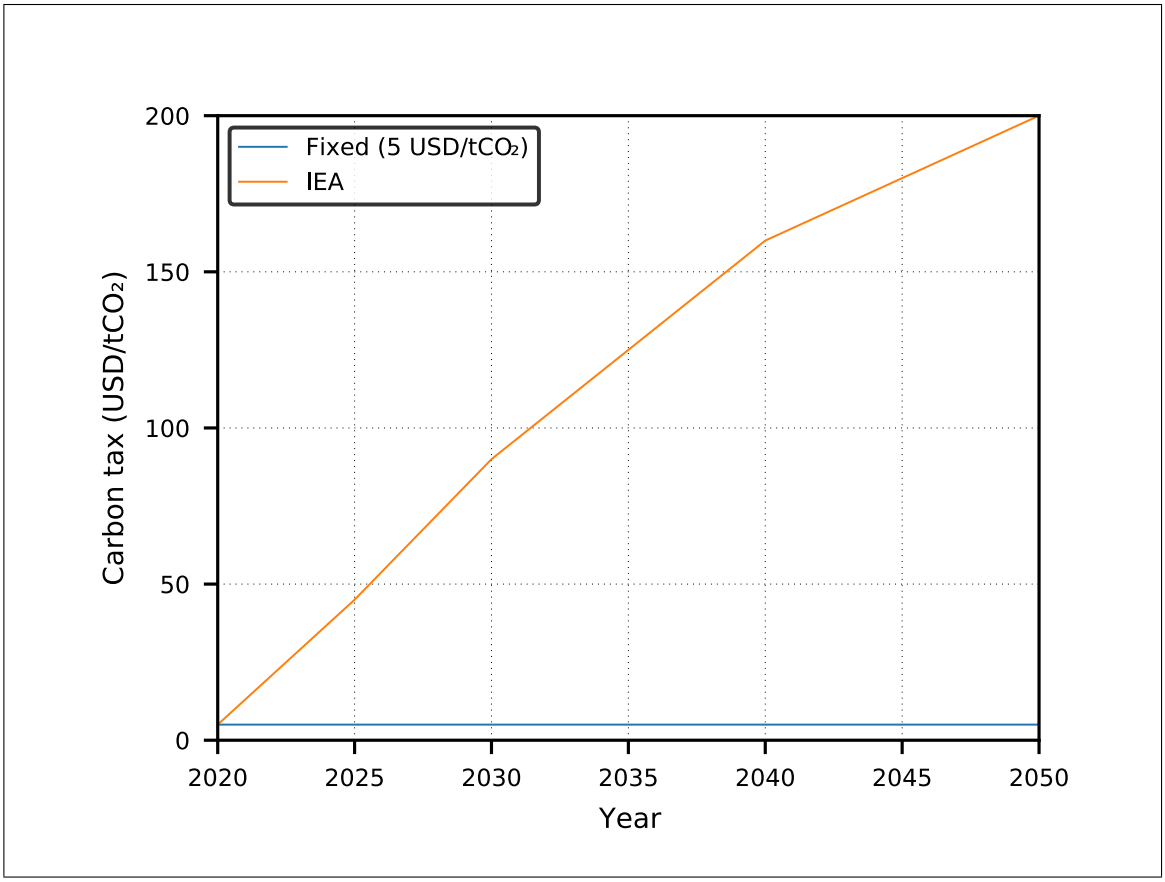

Figure 3.7. Carbon tax values.
Source: IEA tax based on IEA (2021d), all rights reserved.
Note: The IEA tax is used solely in the BHT and H_2EXPHT scenarios.

Table 3.6. Scenarios studied.

Scenario	Carbon tax (USD/tCO_2)	100% RE mandate	H_2 exports
Baseline (B)	Fixed (5)	No	No
Baseline w/higher tax (BHT)	IEA (5-200)	No	No
100% RE by 2050 (RE2050)	Fixed (5)	2050	No
100% RE by 2040 (RE2040)	Fixed (5)	2040	No
Hydrogen exports (H_2EXP)	Fixed (5)	No	Yes
Hydrogen exports high tax (H_2EXPHT)	IEA (5-200)	No	Yes
Hydrogen exports high pipeline cost (H_2EXPHPC)	Fixed (5)	No	Yes

Note: RE = Renewable energy.

4. RESULTS AND DISCUSSION

In this section, we discuss the obtained results of the long-term planning exercise for the Chilean energy system. The model was implemented using the Julia language, with the JuMP environment (Dunning et al., 2017), and the Gurobi solver.

4.1. Investments

Hereafter, we analyze the case study outcomes with regard to investments in hydrogen and electricity production, transport, and storage. Figure 4.1 and Table 4.1 illustrate the installed generation capacities by 2050 across all studied scenarios. The total generation capacity grows from around 26 GW in 2020 to almost 95 GW in 2050 in the baseline (B) and 130 GW in H_2EXPHT. These capacities mark increases of over 300% and 400% over the thirty-year horizon, respectively. In that period, peak base demand (electricity demand without electrolysis) grows from 10 to 25 GW, whereas peak electrolysis consumption varies from over 20 GW in B to more than 50 GW with hydrogen exports. Coal power is already fully phased-out by 2050. In B, the capacity mix is dominated by solar PV (56%) and wind power (16%), with CSP barely reaching 1.2% of the total capacity. The shares of all technologies, however, vary across scenarios. On one hand, the comparative installed capacities showcase the effects of the simulated policies in the capacity mix: both a higher carbon tax and a 100% renewable mandate boost increases in CSP, wind, and solar PV capacity, compared with the B scenario. Increased CSP capacity in RE2050 and RE2040 is due to having to compensate for phased-out fossil fuel power capacity that both provides flexibility and reserve capacity. Furthermore, adding hydrogen exports supports CSP investments and nullifies battery deployment, as surplus renewable electricity goes towards additional hydrogen production instead of battery electricity arbitrage, as CSP provides slightly lengthier storage and can also contribute inertia. Similarly, H_2CCGT investments are slightly reduced but still prevail due to their dispatchable generation and inertia contributions. With hydrogen exports, additional capacity in thermal generation (CSP, gas, diesel) is due to higher flexibility and reserve needs.

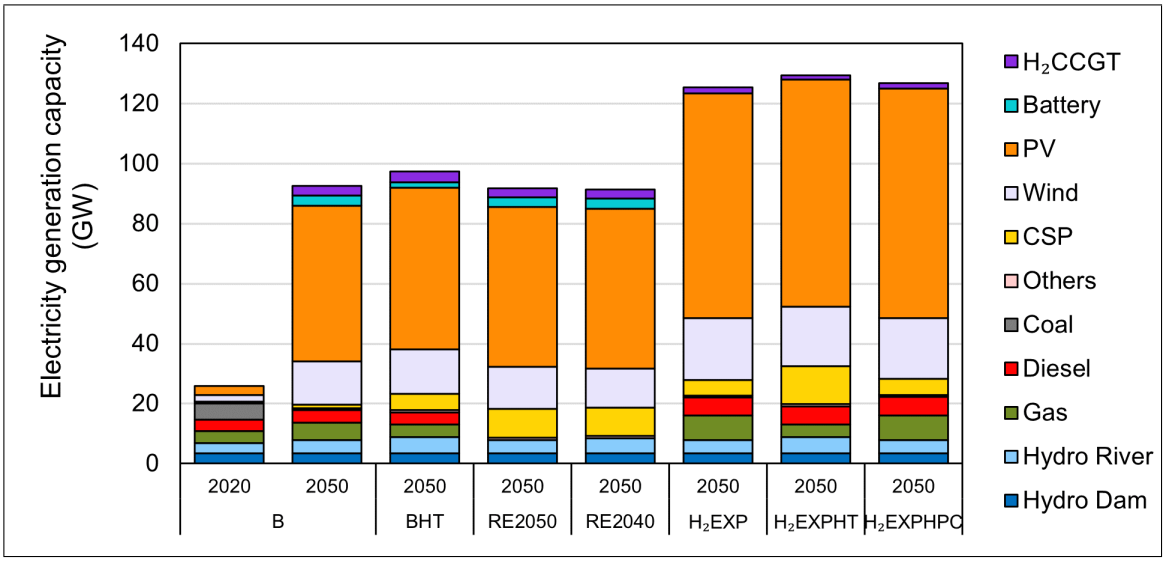

Figure 4.1. Electricity generation capacity comparison by scenario in 2050.

Table 4.1. Comparison of total energy production capacity in 2050 by scenario.

Item (GWel)/Scenario	B	BHT	RE2050	RE2040	H_2EXP	H_2EXPHT	H_2EXPHPC
CSP	1.09	5.39	9.76	9.57	5.36	12.76	5.27
Wind	14.40	14.93	13.82	13.00	20.50	19.71	19.92
PV	51.63	54.02	53.29	53.53	74.68	75.48	76.53
Battery	3.57	1.70	3.20	3.32	0.00	0.00	0.00
H_2CCGT	3.04	3.74	3.07	3.02	1.79	1.18	1.61
Hydropower	7.93	8.92	7.93	8.50	7.93	8.92	7.93
Gas	5.92	4.13	0.00	0.00	8.14	4.13	8.17
Diesel	4.12	4.12	0.00	0.00	6.24	6.23	6.61
Others	0.61	0.71	0.68	0.71	0.61	0.68	0.61
Total	**92.29**	**97.66**	**91.75**	**91.65**	**125.24**	**129.09**	**126.65**
Electrolysis	24.14	29.21	50.57	50.34	50.17	25.98	25.80

The studied policies also impact intermediate investments throughout the horizon. Figure 4.2 shows that incremental capacity needs are mostly met with solar PV and wind power. Further, 100% renewable mandates in 2050 and 2040 augment investments in CSP plants by 2050 and 2040, respectively, directly linking their addition to the phase-out of fossil fuel generators. As previously discussed, the RE2040 and RE2050 scenarios have

practically the same generation capacities by technology in 2050; the only difference is when the CSP investments are made, but not their magnitude. We also note that the higher carbon tax in BHT also increases CSP capacity additions by 2040, supporting gas-to-CSP switching. Hydrogen exports anticipate and augment investments in solar PV, wind, and CSP capacity, while also increasing fossil fuel power additions aimed at ensuring the security of supply in light of the significant additional power demand caused by electrolysis.

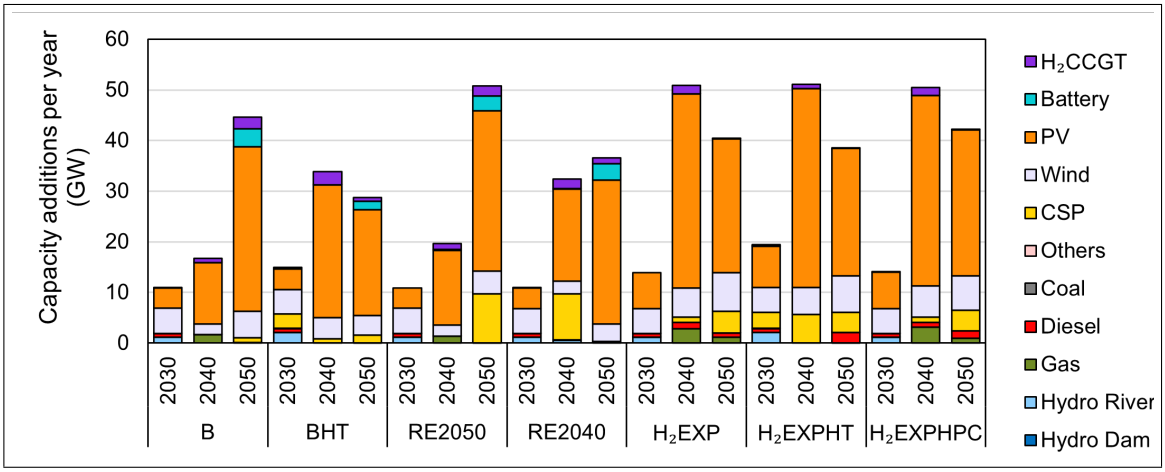

Figure 4.2. Electric capacity additions per year by scenario.
Note: This chart includes both planned and candidate investments.

There is a clear trend across all scenarios that the most cost-effective location for hydrogen production corresponds to the northern regions of the country, particularly located in nodes 5, 7 (Antofagasta region) and nodes 2, 3 (Tarapacá region). From a system perspective, centralizing the majority of hydrogen supply in the northern regions would be the most economically efficient choice. That hydrogen would then be delivered to either neighboring nodes or to more distant demand poles that will consume large amounts of hydrogen, such as the Metropolitan Region. Notably, practically no electrolysis capacity is installed in this region (nodes 15-16), despite having almost 25% of total domestic hydrogen demand by 2050. The higher pipeline costs in H_2EXPHPC shift practically all electrolysis capacity in the northern regions towards node 7 (the export node closest to the Mejillones port).

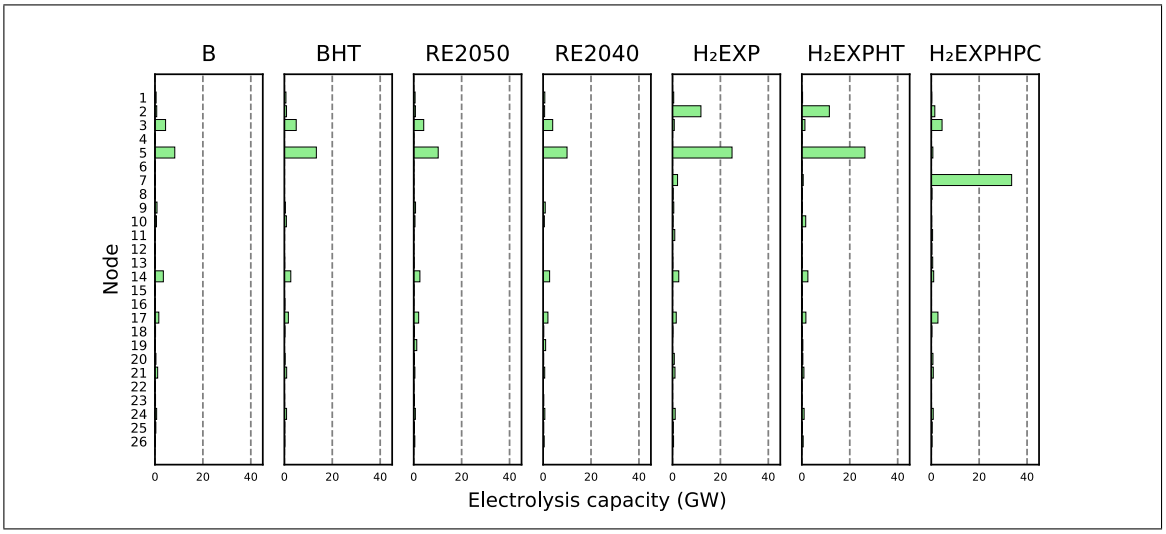

Figure 4.3. Electrolysis capacity installed in 2050 by scenario.
Note: The nodes are ordered from north (top) to south (bottom).

Table 4.2 shows the results across all studied scenarios in 2050 for energy storage capacity. As previously discussed, both climate policies and hydrogen exports tend to reduce battery capacity in favor of other flexible technologies such as CSP (which also contributes inertia) or higher hydrogen production. The opposite happens for hydrogen storage, as increased hydrogen production supports higher storage investment requirements. Batteries would be mostly located in northern and central nodes of the system (see Figure 4.4), showing that they are not exclusively co-located with variable renewable plants (which dominate the northern regions). The largest hydrogen storage assets (Figure 4.5) would be co-located with electrolyzers in the northern regions, but overall this technology shows a more distributed geospatial pattern than electric batteries, particularly in the southern regions. H_2CCGT units would be deployed significantly, mostly co-located with hydrogen production in the north (Figure 4.6).

Table 4.2. Comparison of total energy storage capacity in 2050 by scenario.

Item/Scenario	B	BHT	RE2050	RE2040	H_2EXP	H_2EXPHT	H_2EXPHPC
Electric batteries (GWh)	35.69	17.03	32.02	33.15	0.00	0.00	0.00
Hydrogen storage (kton)	4.07	6.68	7.22	7.21	9.64	11.59	9.74
Hydrogen storage (GWh_{H_2})	135.47	222.39	240.29	240.12	321.12	386.05	324.48

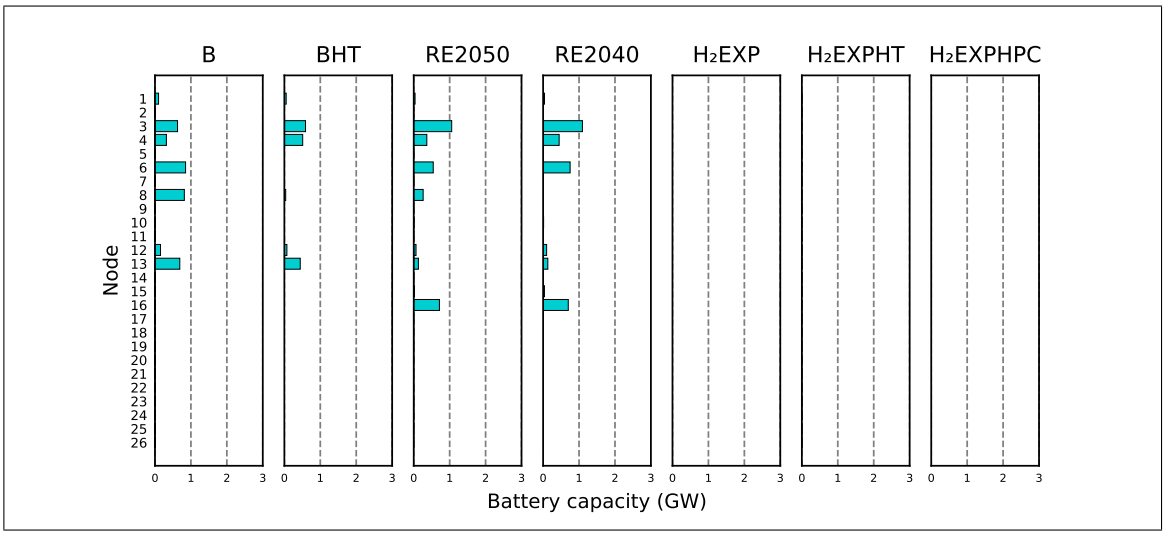

Figure 4.4. Battery capacity installed in 2050 by scenario.
Note: The nodes are ordered from north (top) to south (bottom).

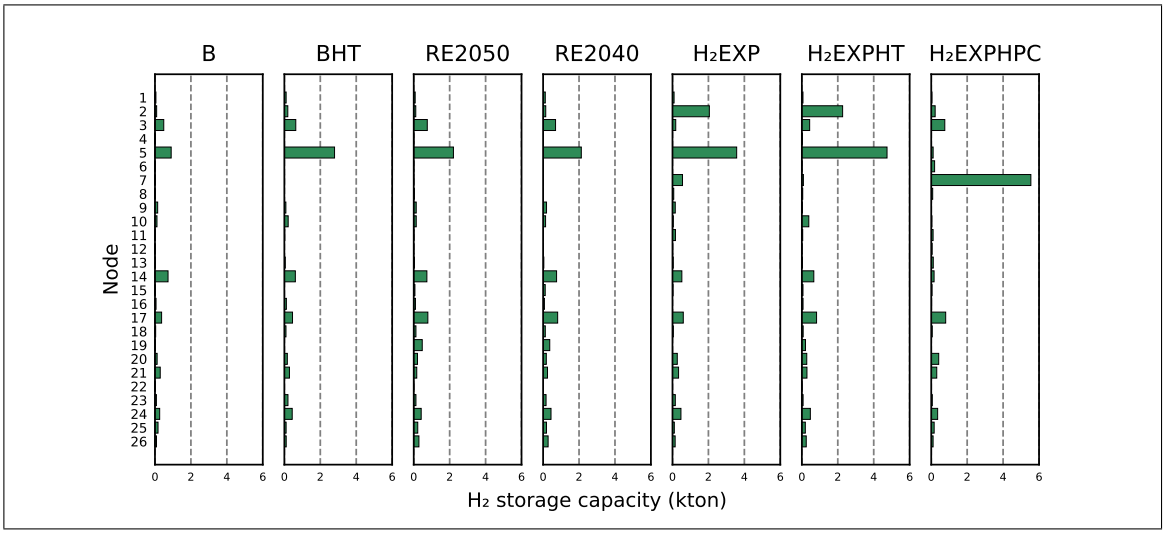

Figure 4.5. Hydrogen storage capacity installed in 2050 by scenario.
Note: The nodes are ordered from north (top) to south (bottom).

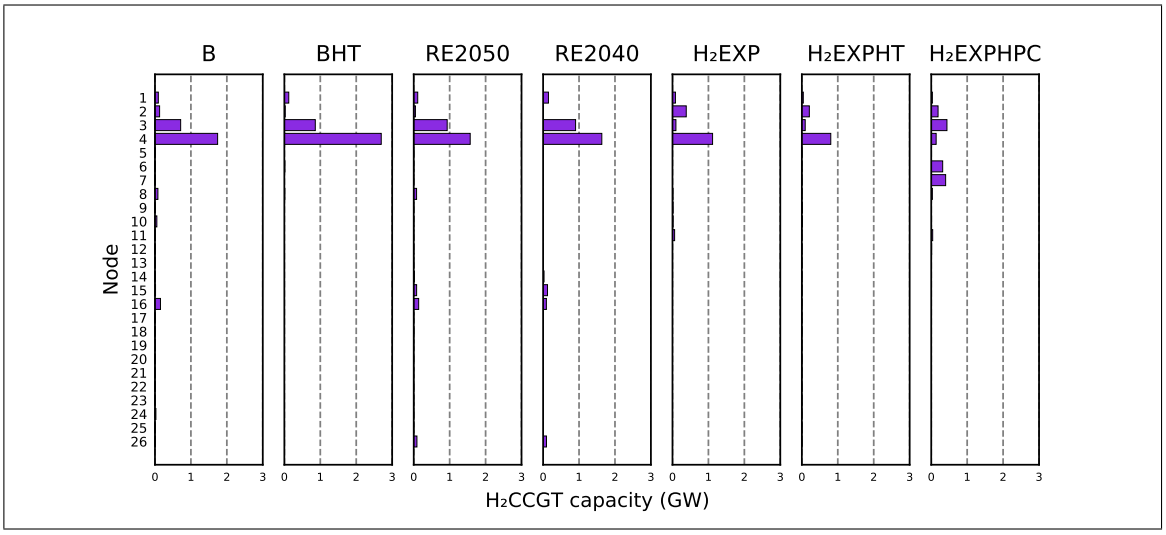

Figure 4.6. H_2CCGT capacity installed in 2050 by scenario.
Note: The nodes are ordered from north (top) to south (bottom).

Table 4.3 compares total energy transport capacities by 2050 across scenarios. The dominant energy transport technology would be transmission lines, with between 9 and 26 times higher transport capacity than hydrogen pipelines, depending on the scenario.

Figure 4.8 shows that very large investments are made in transmission lines, with many corridors surpassing 20 GW of capacity in the scenarios with domestic hydrogen demand only, and over 40 GW for some corridors in the hydrogen exports scenarios. Pipeline capacity does not surpass 5 GW without hydrogen exports, but international trade supports significant increases to over 10 GW in some scenarios. H_2EXPHPC shows that increasing pipeline costs by almost 150% causes investments in the 5-7 transport corridor to disappear, meaning that it is now cheaper to produce the hydrogen for exports in node 7 (the northern export node) rather than to transport a significant part from node 5 to 7. Finally, it can be noted that including hydrogen exports triggers larger capacity additions in hydrogen pipelines relative to transmission lines, and that the higher pipeline costs result in more than halving total hydrogen pipeline investments.

Table 4.3. Comparison of total energy transport capacity in 2050 by scenario.

Item/Scenario	B	BHT	RE2050	RE2040	H_2EXP	H_2EXPHT	H_2EXPHPC
Electricity transmission (GW)	290.61	305.36	282.03	281.41	486.55	441.40	493.95
Hydrogen transport (ton/hr)	267.49	292.96	240.07	240.54	1074.72	1093.29	472.14
Hydrogen transport (GW_{H_2})	8.91	9.76	8.00	8.01	35.80	36.41	15.73

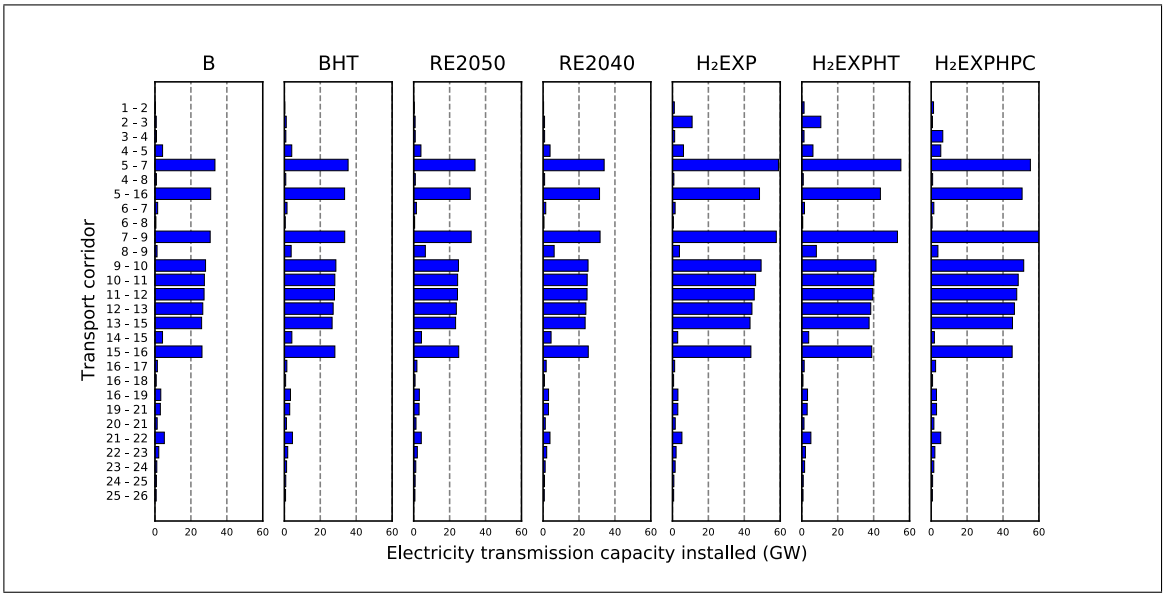

Figure 4.8. Electricity transmission capacity in 2050 by scenario.
Note: The corridors are ordered from north (top) to south (bottom).

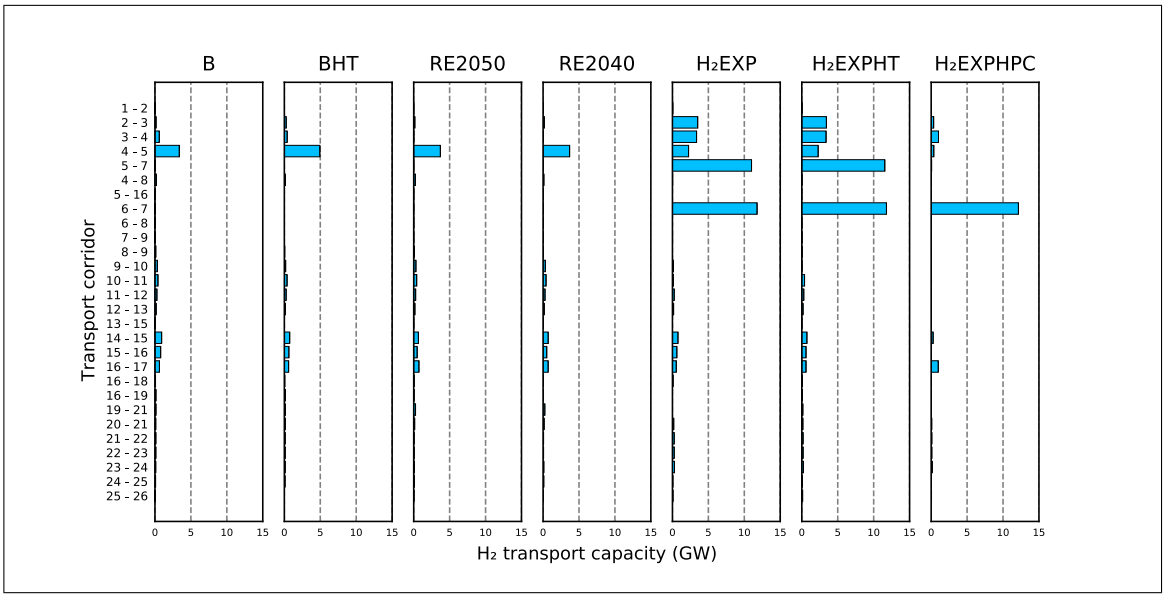

Figure 4.9. Hydrogen transport capacity in 2050 by scenario.
Note: The corridors are ordered from north (top) to south (bottom).

4.2. System costs and emissions

In this section, we discuss and compare the results obtained for system costs and carbon emissions indicators throughout the 2020-2050 horizon.

Both incorporating hydrogen exports and enacting stronger climate policies augment system costs. Table 4.4 compares the system net present value across all scenarios, showing that the majority of the costs are split between investment and variable costs, with investments playing a larger role in the hydrogen exports scenarios. Hydrogen exports cause notable system cost increases of up to 53%, while the 100% renewable mandates augment the total system costs by under 11%. Advancing the 100% renewable mandate to 2040 produces slightly higher costs (versus by 2050) due to increased dispatchable renewables investments in earlier years.

Table 4.4. Comparison of system costs and carbon tax payments by scenario.

Item/Scenario	B	BHT	RE2050	RE2040	H_2EXP	H_2EXPHT	H_2EXPHPC
NPV Total system costs (BUSD)	54.9	62.4	56.3	60.8	76.9	83.9	77.3
NPV Investment costs (BUSD)	22.2	38.6	25.2	34.1	42.1	56.1	42.3
NPV Fixed costs (BUSD)	3.1	7.0	4.0	6.4	6.8	10.9	6.7
NPV Variable costs (BUSD)	29.6	16.8	27.1	20.3	28.1	16.9	28.3
NPV Carbon tax payments (BUSD)	1.7	5.4	1.6	1.4	1.7	5.4	1.7

Note: NPV = Net present value. Carbon tax payments are excluded from the total system costs presented. No revenues from energy trade are considered.

The analyzed climate policies have relevant impacts on the system emissions throughout the horizon, while hydrogen exports decrease the system's total emissions and its emissions intensity, as can be seen in Table 4.5. In 2050 in B, the system would reach about a third of the total 2020 annual CO_2 emissions, showing that, without additional measures, the system would already be set to reduce its emissions. However, to reach near-zero or

zero emissions by 2050, additional climate policies (such as the options discussed here) would be required. Moreover, despite RE2050 and RE2040 reaching zero emissions by 2050, cumulative emissions are reduced by at most a third compared with B, and RE2050 and RE2040 follow an almost identical emissions trajectory to B before 2040 (see Figure 4.10). This suggests that, if drastically reducing cumulative emissions is also meant, a 100% renewable mandate for 2050 may not suffice. Additionally, as a result of incremental electricity demand for hydrogen production met by renewable sources, the export scenarios present slightly lower emissions values than B, with notably lower emissions intensity favoring both electricity and hydrogen production. However, the prevalence of gas generation is only removed with climate policies, which would be particularly desirable if hydrogen and/or electricity are intended to be traded as low or zero-carbon energy.

Table 4.5. Comparison of carbon emissions indicators in 2050 by scenario.

Item/Scenario	B	BHT	RE2050	RE2040	H_2EXP	H_2EXPHT	H_2EXPHPC
Annual emissions ($MtCO_2$)	9.3	1.0	0.0	0.0	8.7	0.8	9.0
Cumulative emissions ($MtCO_2$)	609.3	261.4	551.3	407.0	583.9	261.3	587.4
Emissions intensity (gCO_2/kWh_{el})	39.5	4.1	0.0	0.0	28.1	2.4	28.8
Hydrogen carbon content ($kgCO_2/kgH_2$)	1.78	0.19	0.00	0.00	1.26	0.11	1.29

Notes: The calculation of the emissions intensity omits the discharge of electric batteries. The hydrogen carbon content is calculated based on the electricity consumption for hydrogen production in 2050 and the resulting electricity emissions intensity for that year.

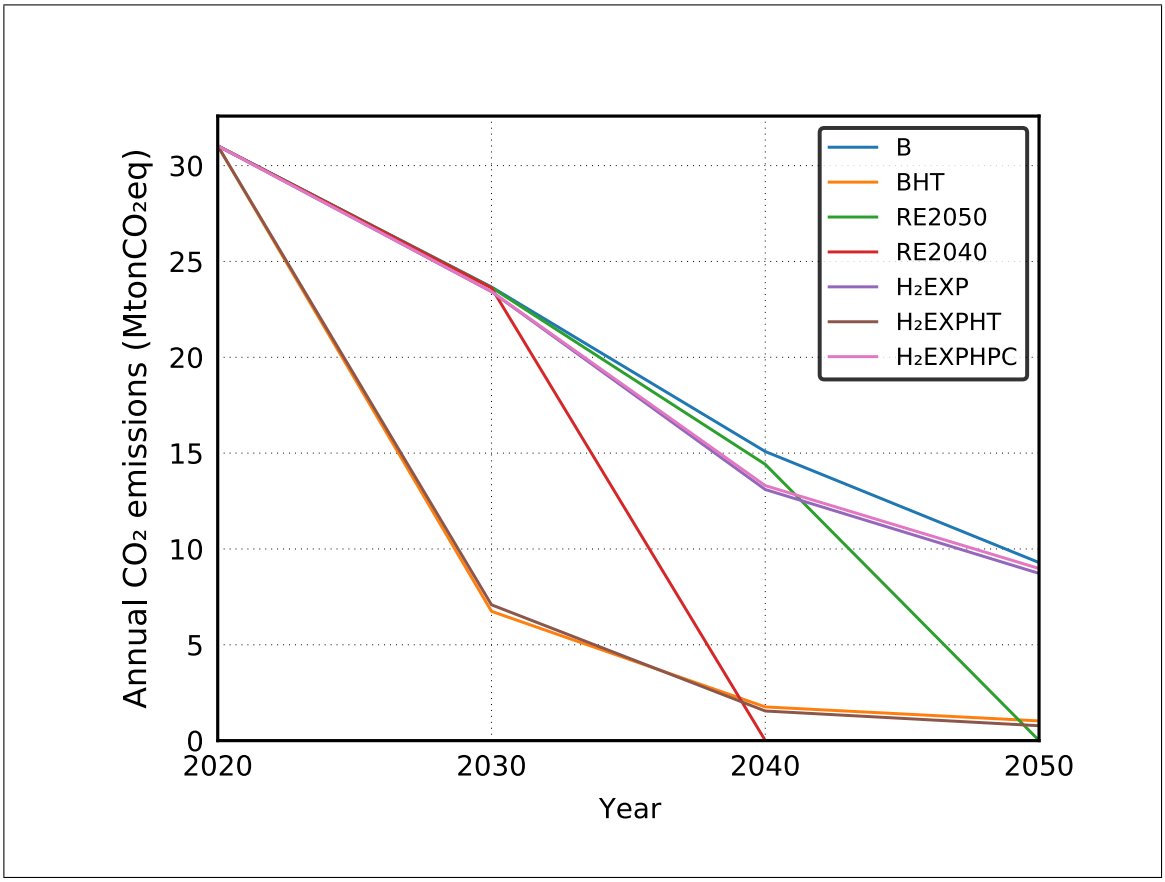

Figure 4.10. Annual CO_2 emissions trajectories by scenario.

4.3. Hydrogen and electricity production costs

In this section, we discuss the outlook of hydrogen and electricity supply prices in light of the studied scenarios. All prices presented are volume-weighted averages (demand or generation, depending on the case).

By computing the dual values of the energy balance constraints, we obtain the marginal cost to supply an additional energy unit. Considering that currently the Chilean electricity market is based on marginal-cost pricing (Muñoz et al., 2021), we use these indicators to provide us with insights into the future electricity prices and to compare the effects caused by different scenarios relative to the baseline. Similarly, we use these results to assess the

future hydrogen market prices. In both cases, we calculate the marginal cost including all network components (not only operational marginal generation costs, but also investments, for example). This reflects overall energy production and delivery costs better, particularly for electricity, as high integration of low-marginal-cost renewables such as solar PV and wind occurs. Given the linear interpolation utilized in the objective function of the model to estimate the total costs throughout the horizon, scaling factors were used to correctly calculate the prices (see Appendix B).

The estimated outlook for electrolyzer- and end-user-perceived electricity prices is presented in Figures 4.11 and 4.12. First, these results show that both the higher carbon tax and the 100% renewable mandates produce little variations in the expected electricity prices by 2050. Second, it is worth noting that adding hydrogen exports to domestic demand, making total hydrogen demand around 3.67 times that of the baseline case, and electricity demand 1.57 times the demand in that same case, notably decreases average electricity prices for typical end-users by up to 1%. Recalling that hydrogen exports increase total system costs, it can be noted that these higher electricity costs are passed on to flexible electrolysis production throughout the full studied period, as electrolysis-consumption-weighted average prices by 2050 are up to 59% higher than those in the baseline case. That increase can also be linked to additional CSP capacity that is installed in the hydrogen exports scenarios. This cross-subsidy-like effect contributes to end-user electricity prices remaining stable between 44 and 46 USD/MWh throughout 2030-2050, always above electrolyzer-perceived prices. Finally, we highlight that adding hydrogen exports also contributes to reduce hourly price deviations, as can be noted when comparing Figures 4.13 and 4.14.

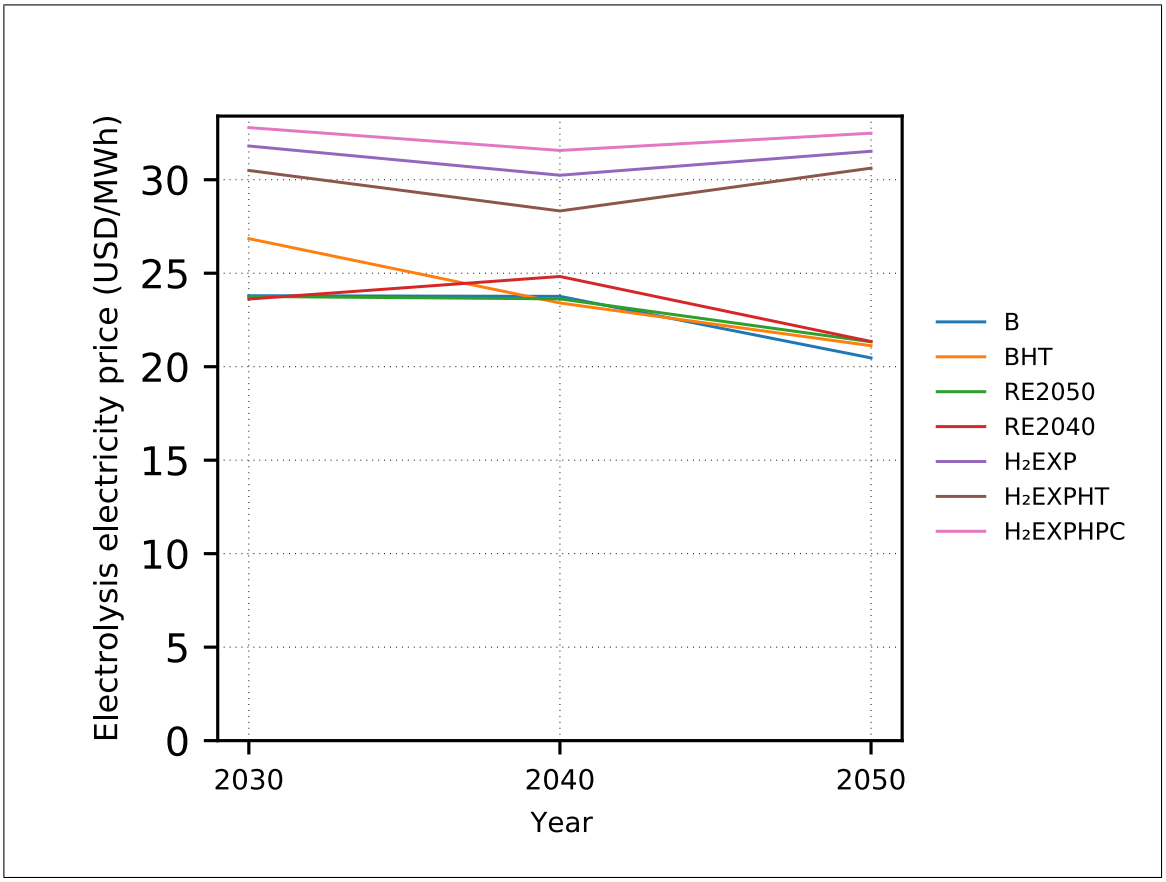

Figure 4.11. Demand-weighted electricity price trajectories for electrolyzers by scenario.
Note: The weights used correspond to the hourly base electricity demand.

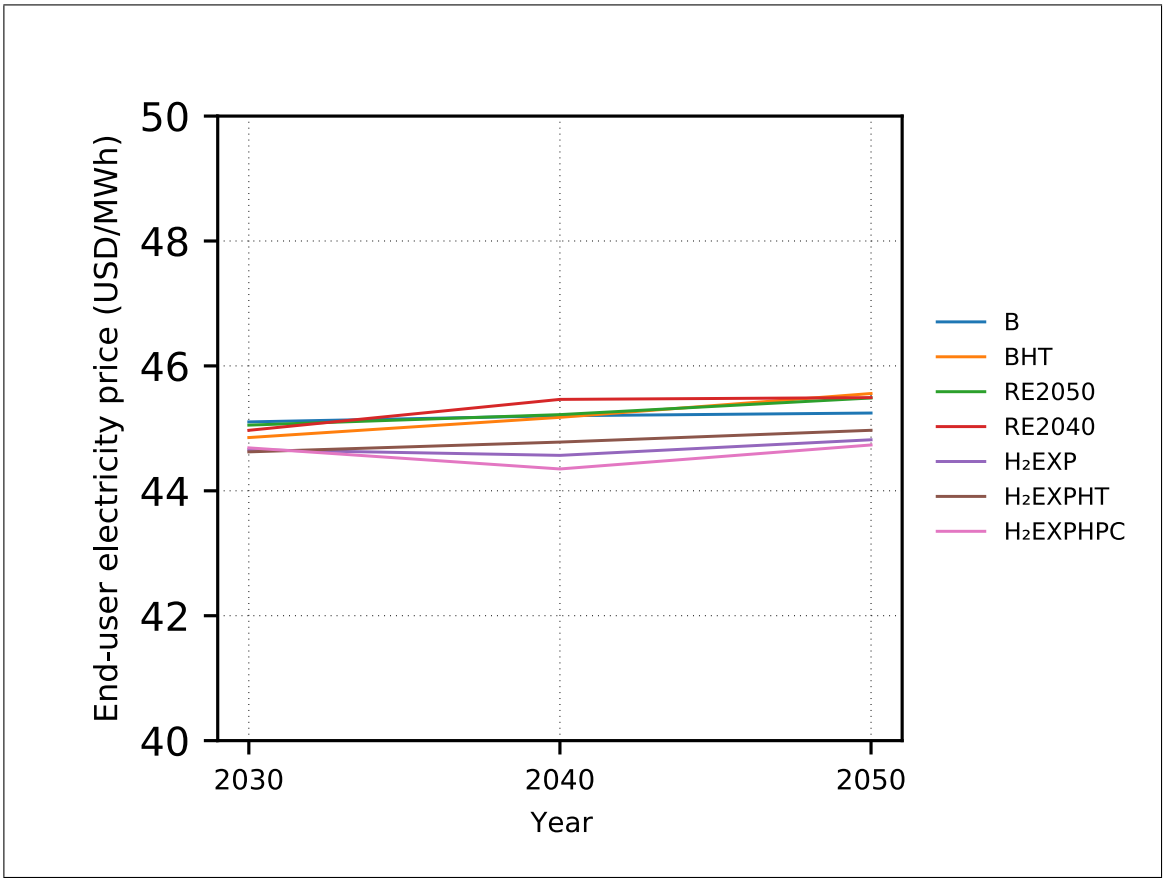

Figure 4.12. Demand-weighted electricity price trajectories for typical end-users by scenario.
Note: The weights used correspond to the hourly base electricity demand.

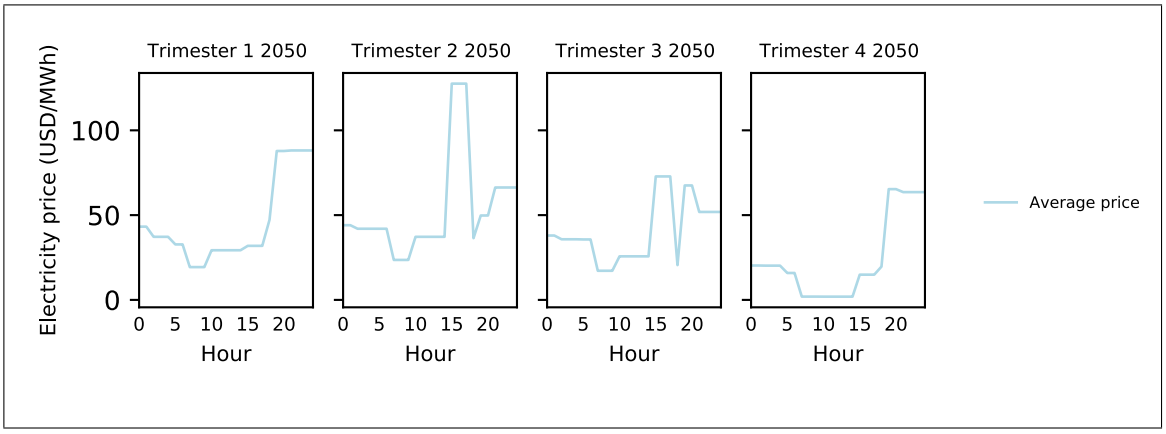

Figure 4.13. Hourly system demand-weighted average price in 2050 in the baseline scenario.

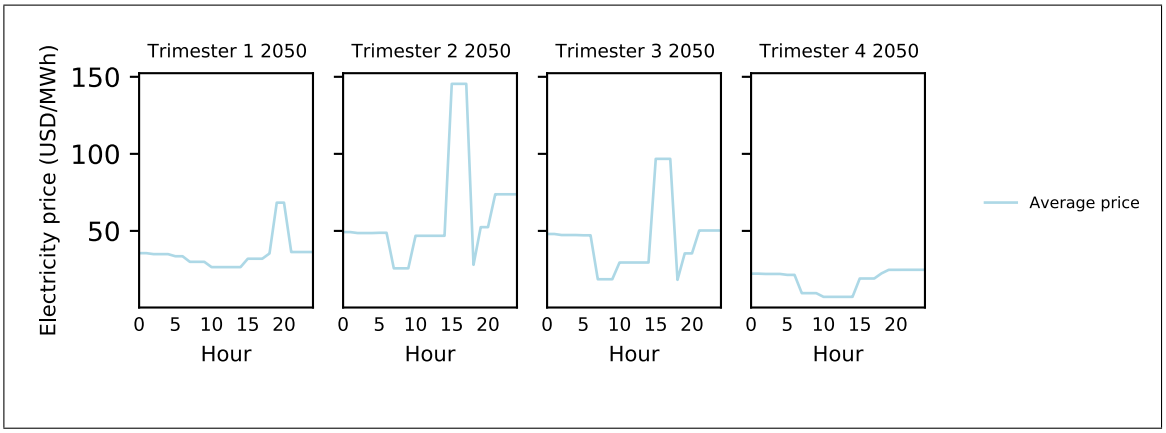

Figure 4.14. Hourly system demand-weighted average price in 2050 in the H_2EXP scenario.

Figure 4.15 shows the hydrogen price trajectory estimates. Hydrogen exports raise the hydrogen prices by up to 39% on the baseline price, markedly higher than for electricity costs. This is directly linked to the electricity price surge for electrolyzers, recalling that energy costs play a large role in hydrogen production costs. Moreover, these hydrogen prices, particularly with hydrogen exports, are somewhat higher than the LCOH target set for 2030 by the Chilean government (Ministerio de Energía, 2020b), to be below 1.5 USD/kgH_2 by that year. This is because the calculation presented in this paper refers

to total system prices, which are expectably higher when also considering transport and storage infrastructure instead of direct production costs only. At the same time, these higher hydrogen prices explain lower investment in H_2CCGT, as they would have around 34% higher variable costs by 2050, based on system average hydrogen prices. However, considering the generation-weighted variable generation costs of these units in the 25-50 USD/MWh range during the 2030-2050 period (see Figure 4.16), H_2CCGT plants could play the role of electricity price-setters that currently thermal plants such as gas generators play in some nodes, particularly in the scenarios with either a higher carbon tax or 100% renewable mandates.

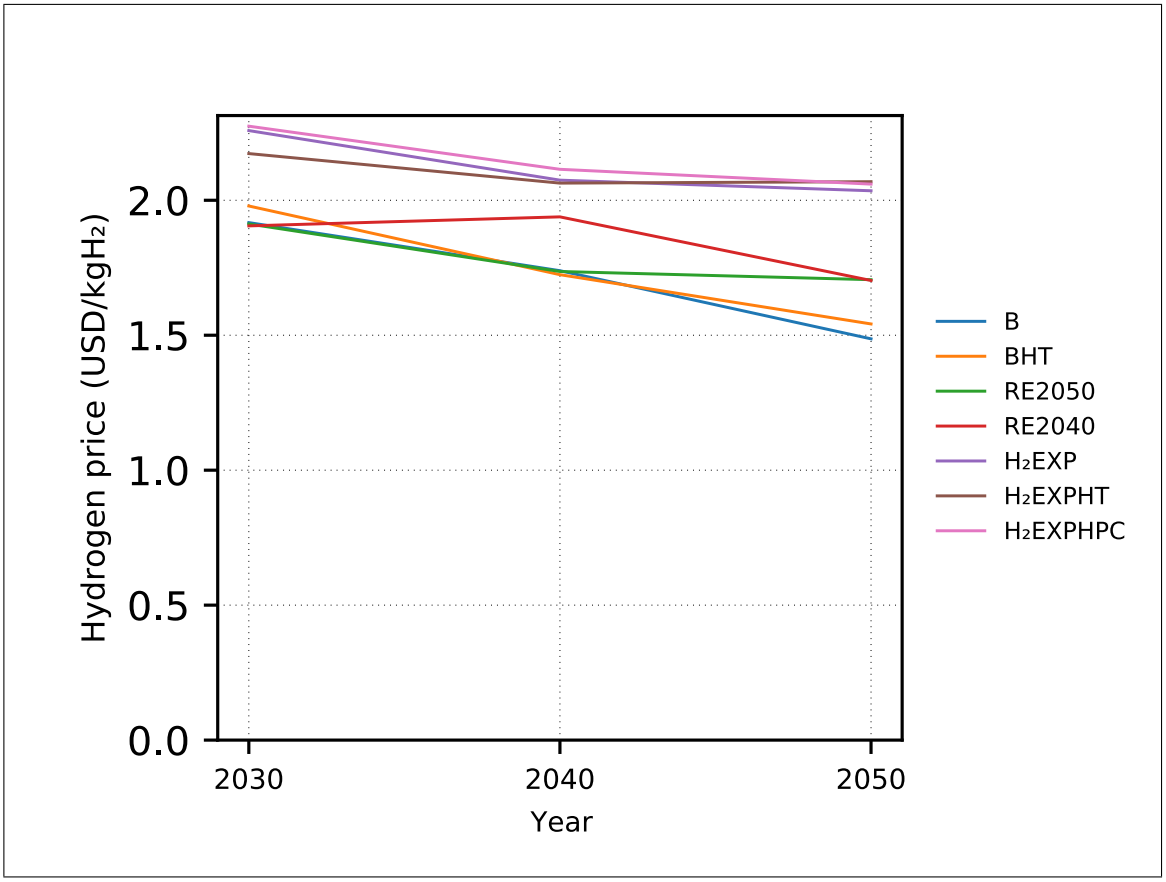

Figure 4.15. Demand-weighted hydrogen price trajectories for electrolyzers by scenario.
Note: The weights used correspond to the hourly hydrogen demand.

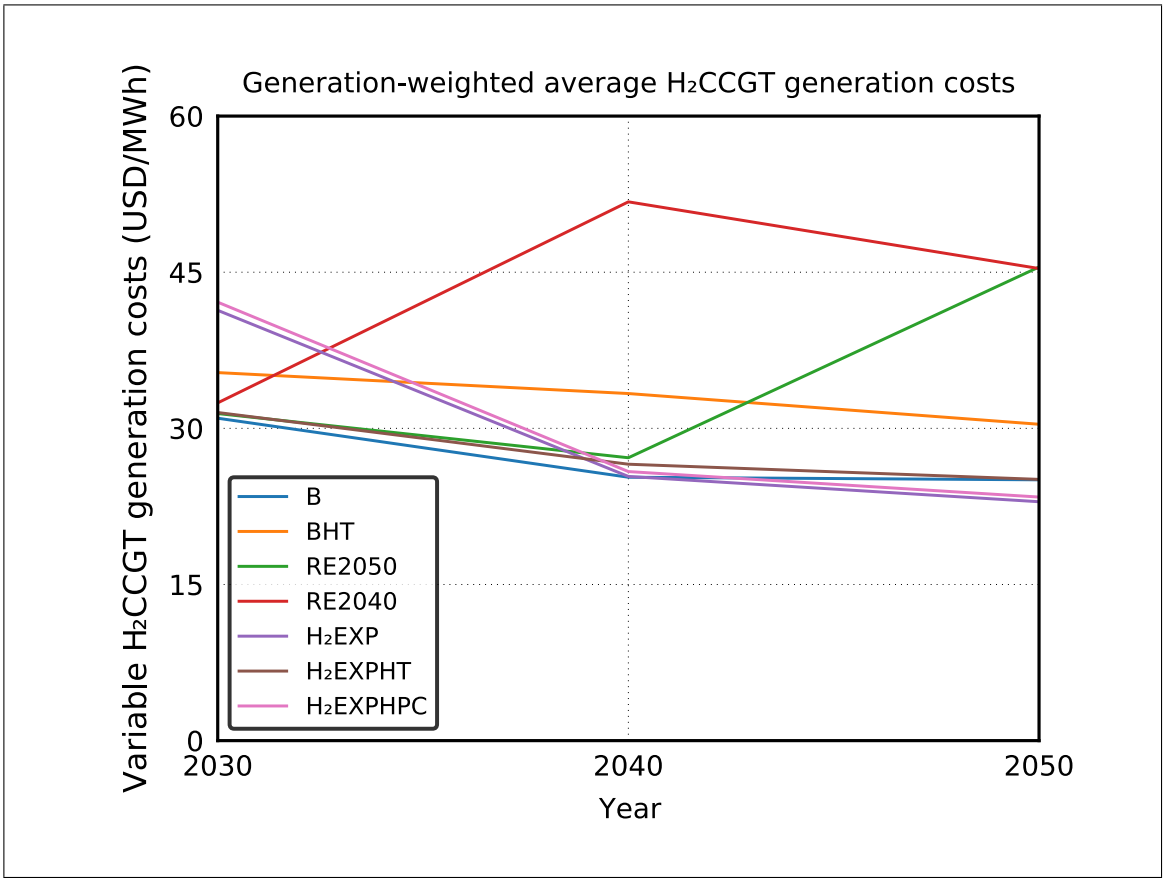

Figure 4.16. Generation-weighted average variable generation costs for H_2CCGT units (including fuel and non-fuel variable costs).

4.4. Operational aspects

4.4.1. Energy production, storage and demand

A discussion of operational aspects is presented in this section, ranging from electricity and hydrogen production, storage, and demand, to hydrogen exports and electrolysis water use.

The system is set to transition from large shares of thermal and hydropower generation towards dominant renewable output, particularly solar PV and wind power. Total generation grows from 80 TWh in 2020 to 244 TWh in 2050 in B (Figure 4.17) and 320 TWh

in H_2EXPHT. In B, incremental energy demand is mostly met by solar PV, wind, CSP, batteries, and H_2CCGT, but also gas generation. In terms of the generation mix, solar PV and wind power generate over two-thirds of the electricity in 2050 in the baseline scenario (see Figure 4.19). This varies significantly from the generation mix of 2020, when coal-fired generation had a share of 38% in our simulation, making it the dominant technology in 2020. Figures 4.18 and 4.19 show two key insights: first, that extra hydrogen export demand is supplied solely with renewable output (solar PV, wind, CSP and hydropower), without incurring in additional fossil generation. Second, however, despite the additional demand that could be met exclusively via renewables, to phase out part or all fossil power such as gas generation by 2050, either a high carbon tax or a 100% renewable mandate would be required.

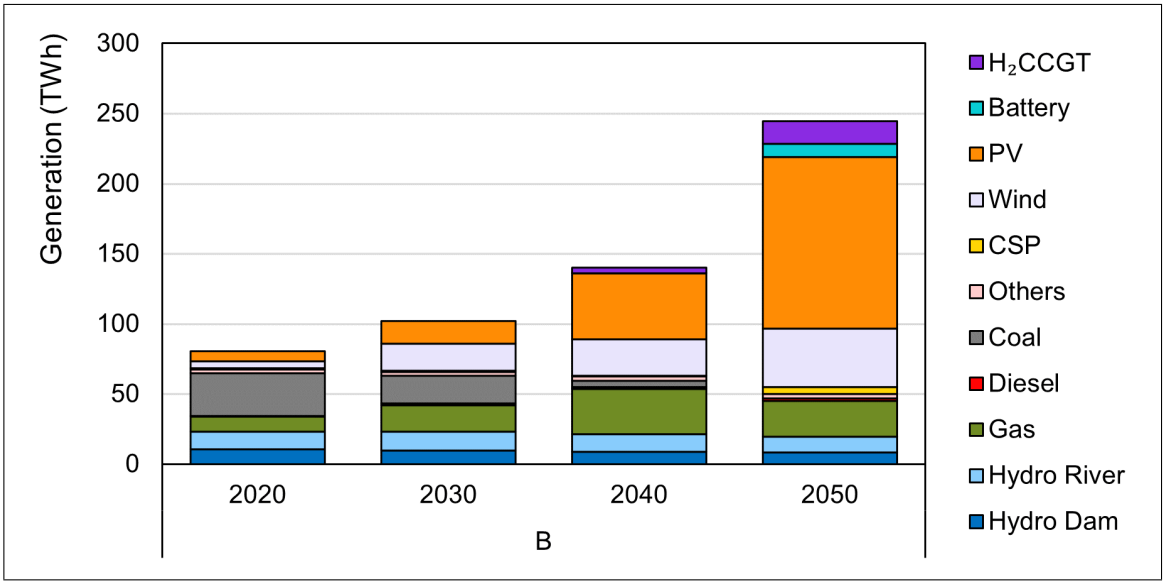

Figure 4.17. Electricity generation evolution in the baseline scenario.

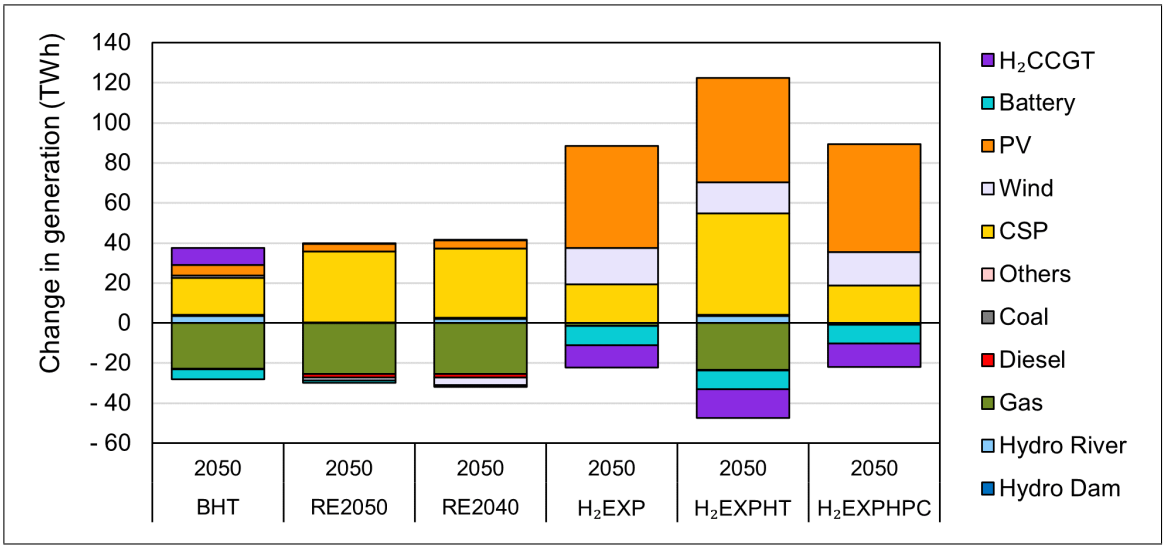

Figure 4.18. Electricity generation in 2050 compared to the baseline scenario.

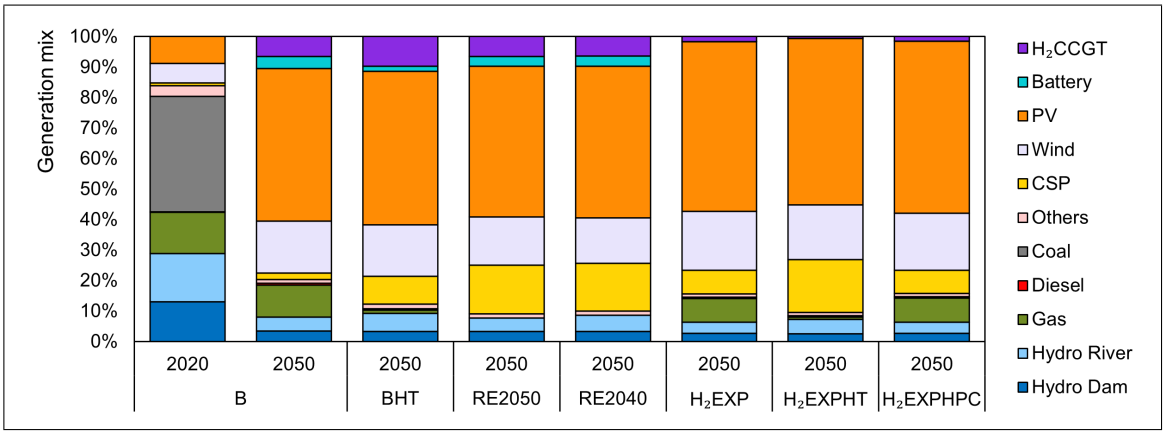

Figure 4.19. Electricity generation mix in 2050 by scenario.

The aforementioned changes in the electricity generation mix translate into varying hourly generation and demand profiles, which are presented based on the intermediate day of each trimester. In 2020, coal, hydropower, and gas are the main suppliers of electricity throughout the day, with solar PV providing a reduced share of electricity (only during daylight hours) and CSP providing an even smaller (but rather constant) supply (see Figure 4.20). By 2050, we observe a much higher ramp-up in generation due to the dominance

of solar PV in the generation mix in the baseline scenario, joined by other low-carbon and fossil fuel power sources (see Figure 4.21). Hydrogen exports trigger larger variable renewable generation, as well as slightly higher CSP generation to provide flexibility and inertia (see Figure 4.22). Flexible low-carbon generation technologies such as CSP, batteries, and H_2CCGT increase their relevance under 100% renewable mandates (see Figure 4.23). Finally, as for the electricity demand to produce hydrogen, our results show a strong linkage between solar resource availability, as electrolytic hydrogen production is mostly carried out during daylight hours (see Figures 4.24 and 4.25), with slightly higher production during nighttime in the export scenarios due to additional CSP output.

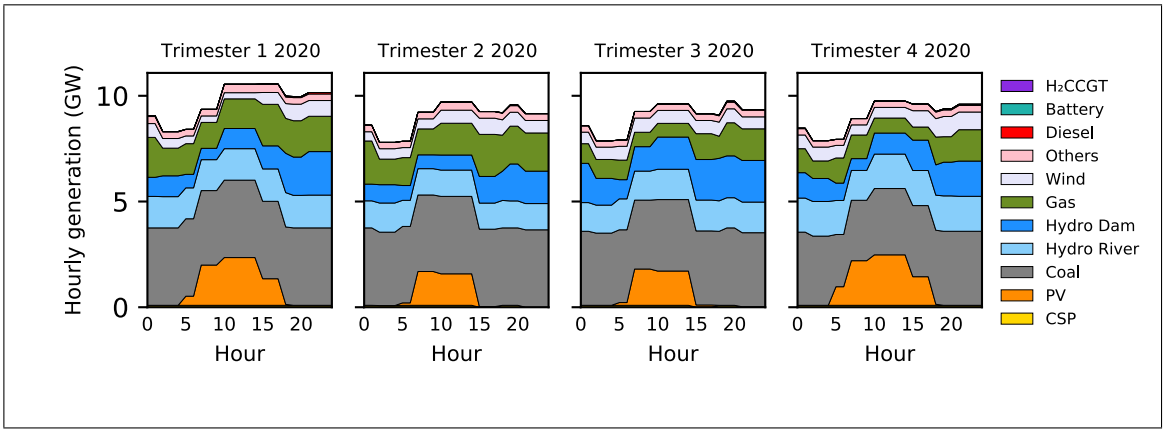

Figure 4.20. Hourly generation in 2020 in the baseline scenario.

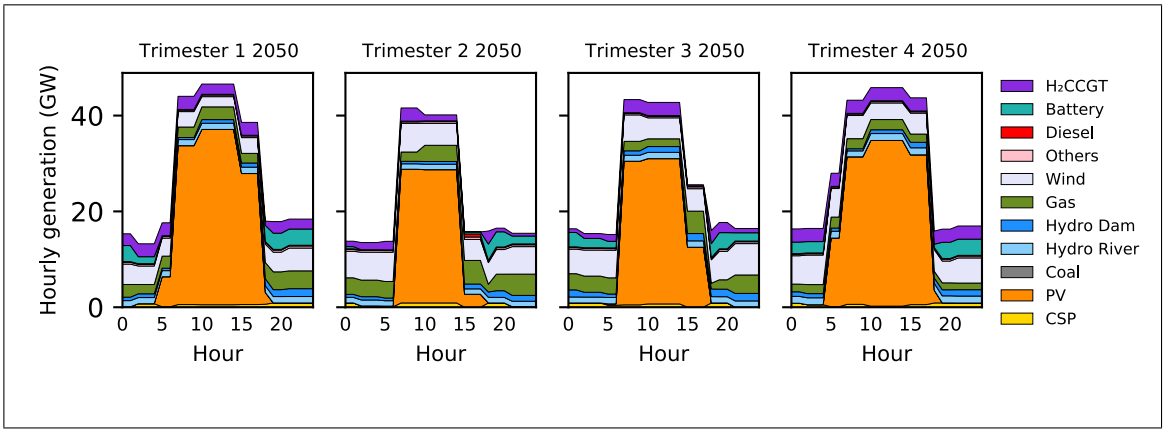

Figure 4.21. Hourly generation in 2050 in the baseline scenario.

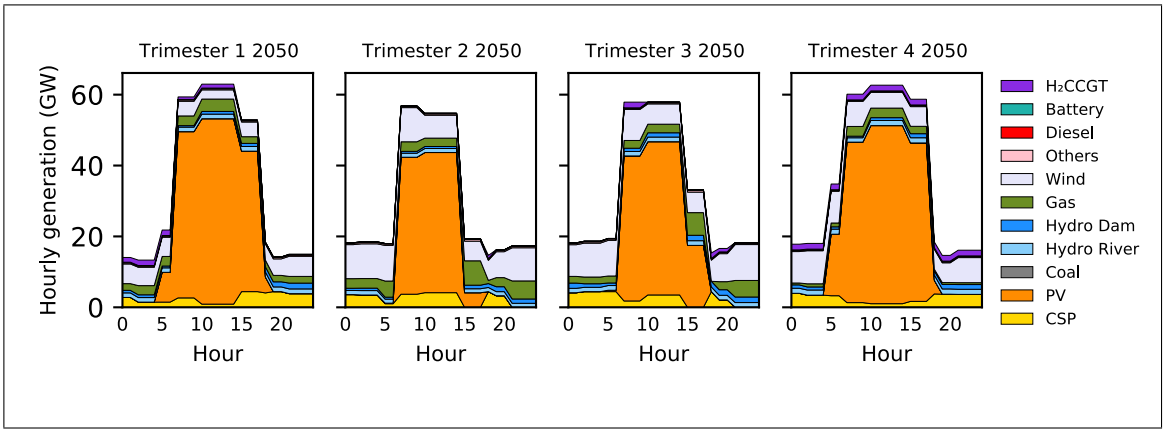

Figure 4.22. Hourly generation in 2050 in the H_2EXP scenario.

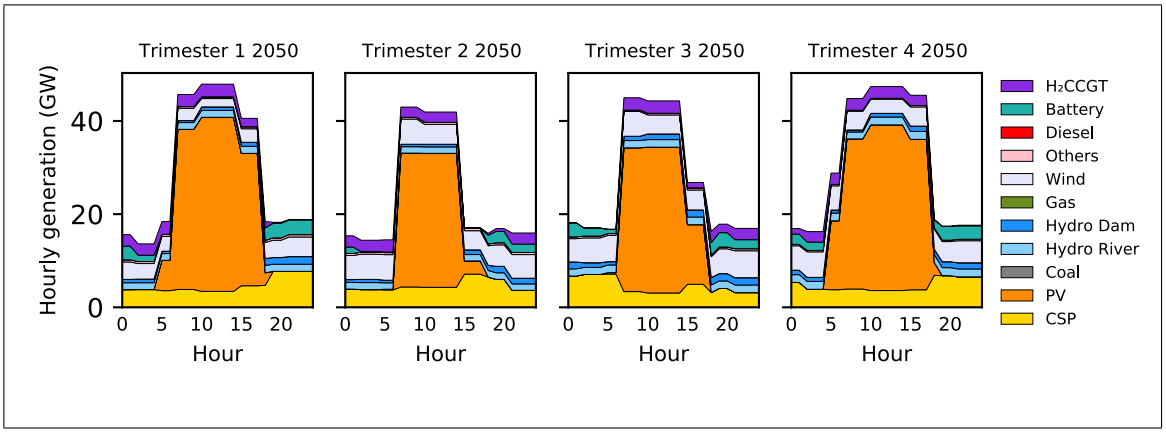

Figure 4.23. Hourly generation in 2050 in the RE2040 scenario.

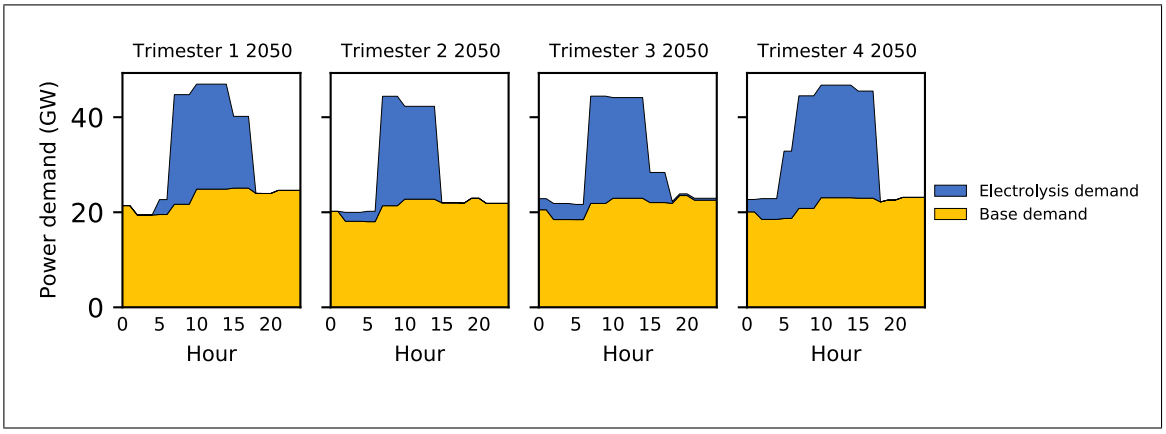

Figure 4.24. Hourly electricity demand in 2050 in the baseline scenario.

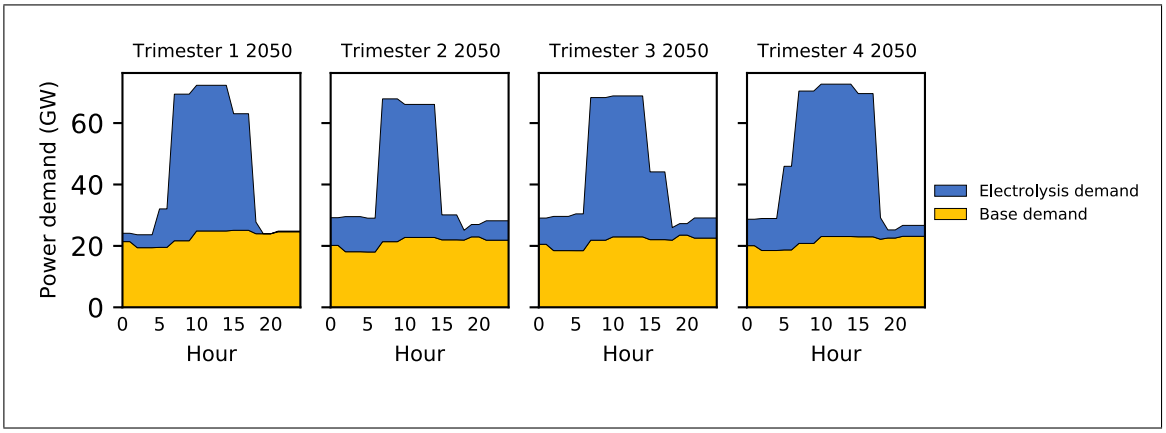

Figure 4.25. Hourly electricity demand in 2050 in the H_2EXP scenario.

Finally, two key insights can be drawn from the model's solution regarding hydrogen exports and storage. First, even though the model can freely allocate the distribution of hydrogen exports between nodes 6, 15, and 20, in all hydrogen exports scenarios over 99% of it is allocated in node 6, closest to the Mejillones port and much closer to most of the solar PV capacity than the other two ports. Second, it can be seen in Figure 4.26 that, taking advantage of the increased solar irradiation in the Southern Hemisphere's summer months, hydrogen is stored on a seasonal basis, peaking at over 4 times in its highest inventory level compared to its lowest throughout the year.

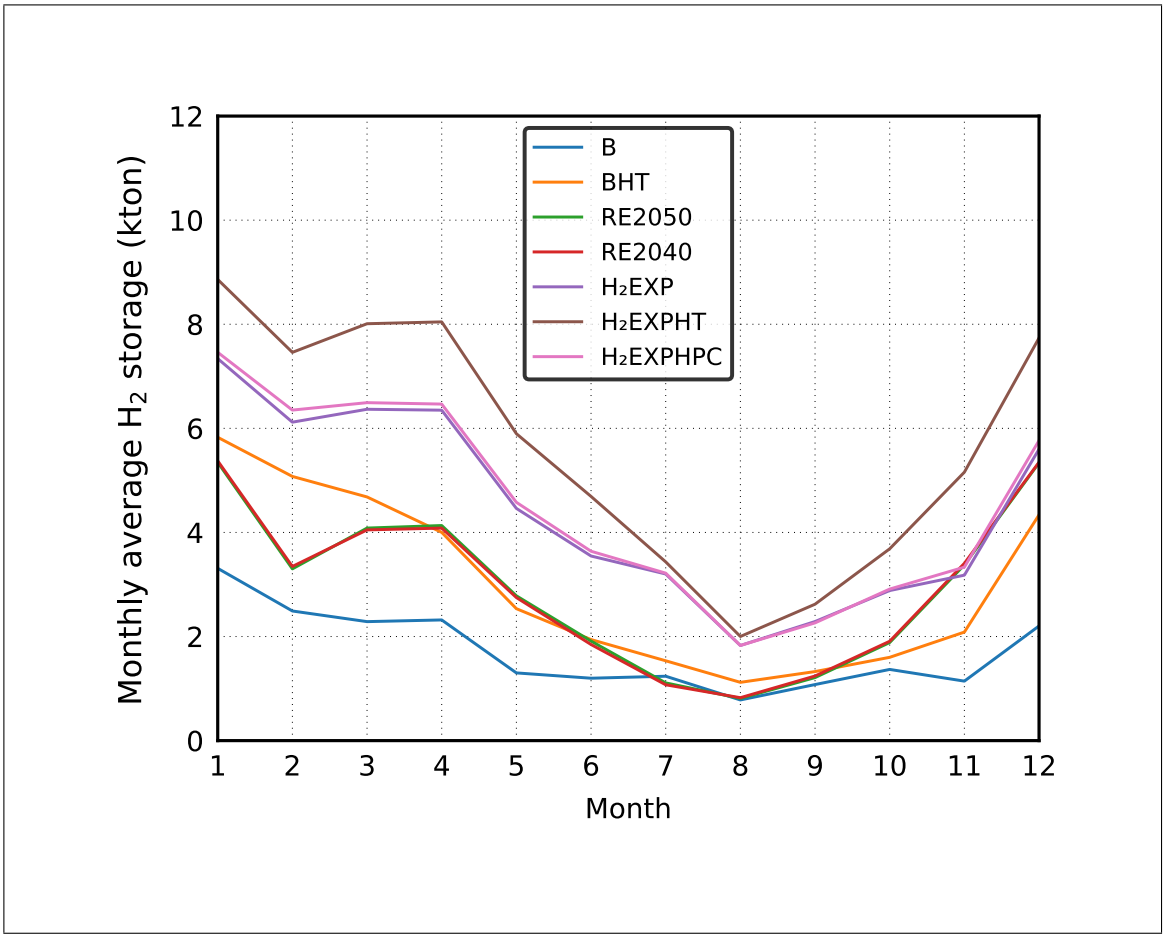

Figure 4.26. Average monthly hydrogen inventory in 2050 by scenario.

4.4.2. Water consumption

Large-scale electrolytic hydrogen production can cause concern due to the stress on water resources that Chile currently has. According to the World Resources Institute (Hofste et al., 2019), Chile had the 18th-highest water stress ranking among a large list of countries analyzed. To tackle water scarcity in Chile, desalination has been one of the solutions considered, with over 5000 lt/s of desalination capacity already deployed in the country for industrial and mining operations (GIZ et al., 2020).

Directly correlated with electrolysis deployment, water use is set to be largely concentrated in northern areas of Chile. With hydrogen exports, total annual water use for hydrogen production by 2050 would reach around 46 m^3 (see Table 4.6). This represents under 0.5% of total annual national water demand, estimated to have been around 9500 million m^3 in 2015 (Osorio-Aravena et al., 2021). Meanwhile, the equivalent average water flow would be just below 1500 lt/s, around a quarter of the current installed desalination capacity for industrial and mining operations (GIZ et al., 2020).

Despite the small share that the expected electrolysis water use would have over total water demand, it could still be a cause of concern, given the country's worsening water stress outlook, particularly if the incremental water demand is partially (or fully) met via water desalination. While some studies claim that the negative environmental impacts of water desalination could be controlled (Miller et al., 2015; Pistocchi et al., 2020; Herrera-León et al., 2022), other studies affirm that there are socio-environmental impacts that still require proper solutions in Chile (Campero et al., 2021; Odell, 2021; Alvez et al., 2020).

Table 4.6. Comparison of annual water consumption for hydrogen production in 2050 by scenario.

Item/Scenario	B	BHT	RE2050	RE2040	H_2EXP	H_2EXPHT	H_2EXPHPC
Annual water consumption (million m^3)	19.65	24.09	21.55	21.39	46.15	45.91	46.00
Annual water consumption (lt/s)	623.09	763.83	683.37	678.18	1463.39	1455.65	1458.65

The water consumption estimates are based on an assumed electrolysis water consumption of 10 lt/kgH_2.

5. CONCLUSIONS

5.1. Conclusions and policy implications

In this paper, we carry out a long-term analysis to provide an outlook for the most cost-effective evolution of the Chilean power system integrated with a hydrogen network, from 2020 to 2050. We propose a new linear optimization model that builds up on existing models in the literature (including the long-term planning exercise of the Chilean Ministry of Energy) to analyze the impacts of a variety of policies and hydrogen demand scenarios. The model optimizes all investment and operational variables and reflects the outcome of a competitive market. This study presents the first assessment of the optimal evolution of the integrated hydrogen-electricity network in Chile considering domestic hydrogen consumption, international hydrogen exports and climate policies, including a representation of essential aspects such as electricity reliability constraints, intra-day and seasonal energy arbitrage, and several energy production technologies. Our proposed model also allows to freely allocate electrolyzer investments on a temporal and geographical scope, and incorporates hydrogen transport and storage. We analyze scenarios considering hydrogen demand variations, carbon pricing, and 100% renewable mandates, drawing several conclusions from our analysis.

First, our results show that, even in the baseline scenario, with domestic hydrogen demand only, a constant carbon tax of 5 USD/tCO_2 and without a 100% renewable generation mandate, it could be the most cost-effective solution to have an integrated energy system that, by 2050, produces about a third of its 2020's electricity-related emissions. The system would have high shares of solar PV and wind generation, together with hydrogen combined-cycle gas turbines, electric batteries, and concentrated solar power plants. In this scenario, however, gas would still account for over 10% of the electricity generation mix. Part of its output would be replaced by other dispatchable generation technologies such as hydrogen combined-cycle gas turbine units, electric batteries and, to a lesser extent, concentrated solar power plants. By 2050, the estimated annual emissions

of the energy system in the baseline scenario would reach 9.3 $MtCO_2eq$ (compared with around 28 $MtCO_2eq$ in 2020). This means that, under the energy demand and technology costs outlook used in this study, the system should be able to reduce carbon dioxide emissions by about two-thirds in 2020-2050 simply following the most cost-effective trajectory. However, to achieve larger emissions reductions throughout the period, additional policies could be required to phase out fossil fuel generation, such as an increased carbon tax or a 100% renewable mandate. Other market-based policy options to close that emissions gap could include an emissions trading system, or investment subsidies for energy production, storage, and/or transport.

Second, we show that increasing carbon prices and enforcing 100% renewable mandates are powerful tools to reduce cumulative emissions over the 2020-2050 horizon. Although the simulated system in the baseline scenario produces low emissions by 2050, enforcing an increasingly high carbon tax during the period can reduce the total CO2 emissions produced in the complete horizon by over 55%. Implementing a 100% renewables mandate by 2040 can further reduce cumulative emissions, but comes at a premium, raising the net present value of the system costs by almost 11% compared with the baseline scenario. Both increasing the carbon tax and enforcing 100% renewable mandates increase system costs, which means that government action could be needed if it is not intended to transfer these additional costs to end-users of electricity and/or hydrogen.

Third, our results notably show that international hydrogen exports in line with the Chilean Hydrogen Strategy (Ministerio de Energía, 2020b) could enhance renewable integration without necessarily incurring in price surges for typical consumers. On the one hand, we note that the incremental electricity demand for hydrogen export production would be met via renewables, particularly solar PV, which results into a lower systemic emissions intensity relative to our baseline. Notably, the additional hydrogen production make battery investments less necessary, as surplus renewable electricity is destined to produce hydrogen. However, there is still a prevalence of gas generation in the system that

would keep the carbon content of grid-produced hydrogen over 1.2 $kgCO_2/kgH_2$ (if calculated based on the system' average annual electricity mix). How certification schemes are designed in the future will be key to define whether the hydrogen produced is low-carbon hydrogen or not, as in this case the additional generation triggered by electrolysis would be renewable (hence, low-carbon), but at the same time the average electricity mix not fully renewable. On the other hand, this 2.67-times increase in hydrogen demand caused by hydrogen exports (and 57% growth in total electricity demand) in 2050, compared with our baseline, would not result in increased average electricity prices for typical electricity consumers. Prices for these customers would actually decrease up to 1% relative to the baseline scenario. End-users would avoid increases as a side effect of the flexibility of electrolyzers, whose production is allocated in hours with cheap electricity, and therefore causes them to see higher system costs reflected in their prices. Electrolyzers would perceive an average electricity price up to 59% higher than with domestic hydrogen demand only. Given the high relevance of electricity prices in hydrogen production costs, this increase translates into higher hydrogen supply prices from around 1.5 USD/kgH_2 in our baseline scenario to about 2.1 USD/kgH_2 when incorporating hydrogen exports. It remains to be seen if this cost increase could significantly reduce the Chilean hydrogen exports' competitiveness in the international market.

Fourth, from an integrated system perspective, almost all the hydrogen production and storage capacity were deployed in the northern regions of Chile, and this result was robust across all scenarios. Our analysis shows that for the Chilean case, it would be more cost-effective to mostly concentrate hydrogen production in the northern regions and then transport it to the rest of the country. Moreover, practically all exports from the country (excluding the Patagonia region) would take place via the Mejillones port, close to some of the best nodes for solar generation. This poses several challenges for policymakers, as a large deployment of hydrogen and power system assets could mean substantial land use needs and new tenders for additional electricity transmission and new hydrogen transport corridors. Additionally, new or modified regulations and standards will be required

for large-scale hydrogen production, transport, storage, and demand. Addressing socio-environmental concerns, together with fostering social acceptance for hydrogen technologies that will be new to most consumers, will have to be addressed by policymakers to meet energy demand in the country without significantly affecting the ecosystem or human communities, for example, due to the installation of large energy transport corridors, desalination plants or energy production facilities. Other alternatives such as deploying less energy transport capacity in favor of more energy production capacity close to demand hubs could be explored, considering for example that our scenario with hydrogen pipeline costs suggested that co-locating hydrogen production with demand could be a convenient alternative if the relative costs of energy transport result too high.

5.2. Further research opportunities

Various lines of study could be addressed to develop further on our analysis. For example, we focus on large-scale assets and demand and do not study infrastructure investments at the distribution level, which could include technologies such as digital distribution system infrastructure, hydrogen-carrying trucks, and others. Further, as we did not limit the maximum installed capacity for energy transport capacity, a thorough study on the feasibility of investing in large-scale energy transport corridors could be beneficial. In our results, investments in electricity transmission corridors of over 40 GW are made, which, if not feasible, may need to be compensated with higher investments in other energy infrastructure which could lead to increased energy supply costs and changes in the investment portfolio. Moreover, it could be worthwhile to incorporate revenues of hydrogen sales in the system planning. Finally, another important extension for future work is to integrate into the analysis other dynamics that could significantly impact the Chilean integrated network, such as electrification of other end-uses including transport and heat.

REFERENCES

Agora Energiewende and AFRY Management Consulting. (2021). *No-regret hydrogen: Charting early steps for H_2 infrastructure in Europe*. Retrieved from `https://www.agora-energiewende.de/en/publications/no-regret-hydrogen/`

Alvez, A., Aitken, D., Rivera, D., Vergara, M., McIntyre, N., & Concha, F. (2020). At the crossroads: can desalination be a suitable public policy solution to address water scarcity in Chile's mining zones? *Journal of Environmental Management*, *258*, 110039. doi: 10.1016/j.jenvman.2019.110039

Armijo, J., & Philibert, C. (2020). Flexible production of green hydrogen and ammonia from variable solar and wind energy: Case study of Chile and Argentina. *International Journal of Hydrogen Energy*, *45*(3), 1541–1558. doi: 10.1016/j.ijhydene.2019.11.028

Bødal, E. F., Mallapragada, D., Botterud, A., & Korpås, M. (2020). Decarbonization synergies from joint planning of electricity and hydrogen production: A Texas case study. *International Journal of Hydrogen Energy*, *45*(58), 32899–32915. doi: 10.1016/j.ijhydene.2020.09.127

Campero, C., Harris, L. M., & Kunz, N. C. (2021). De-politicising seawater desalination: Environmental Impact Assessments in the Atacama mining Region, Chile. *Environmental Science & Policy*, *120*, 187–194. doi: 10.1016/j.envsci.2021.03.004

Dunning, I., Huchette, J., & Lubin, M. (2017). Jump: A modeling language for mathematical optimization. *SIAM Review*, *59*(2), 295-320. doi: 10.1137/15M1020575

Gacitúa, L., Gallegos, P., Henriquez-Auba, R., Lorca, A., Negrete-Pincetic, M., Olivares, D., ... Wenzel, G. (2018). A comprehensive review on expansion planning: Models and tools for energy policy analysis. *Renewable and Sustainable Energy Reviews*, *98*,

346–360. doi: 10.1016/j.rser.2018.08.043

Gallardo, F. I., Monforti Ferrario, A., Lamagna, M., Bocci, E., Astiaso Garcia, D., & Baeza-Jeria, T. E. (2021). A Techno-Economic Analysis of solar hydrogen production by electrolysis in the north of Chile and the case of exportation from Atacama Desert to Japan. *International Journal of Hydrogen Energy*, *46*(26), 13709–13728. doi: 10.1016/j.ijhydene.2020.07.050

GIZ, Centro de Energía Universidad de Chile, & Ministerio de Energía. (2020). *Identificación de zonas para el desarrollo de proyectos integrales de agua y energía* (Report). GIZ. Retrieved from https://www.4echile.cl/proyectos/descarbonizacion-del-sector-energetico-de-chile/identificacion-de-zonas-para-el-desarrollo-de-proyectos-integrales-de-agua-y-energia/

GIZ, & HINICIO Chile. (2021). *Cuantificación del encadenamiento laboral para el desarrollo del hidrógeno en Chile bajo un escenario de exportación.* Retrieved from https://www.4echile.cl/publicaciones/cuantificacion-del-encadenamiento-laboral-para-el-desarrollo-del-hidrogeno-en-chile-bajo-un-escenario-de-exportacion/

GIZ, & Ministerio de Energía. (2014). *Energías renovables en Chile. El potencial eólico, solar e hidroeléctrico de Arica a Chiloé.* Retrieved from https://biblioteca.digital.gob.cl/handle/123456789/510

Gonzato, S., Bruninx, K., & Delarue, E. (2021). Long term storage in generation expansion planning models with a reduced temporal scope. *Applied Energy*, *298*, 117168. doi: 10.1016/j.apenergy.2021.117168

He, G., Mallapragada, D. S., Bose, A., Heuberger-Austin, C. F., & Gençer, E. (2021). Sector coupling via hydrogen to lower the cost of energy system decarbonization. *Energy & Environmental Science*, *14*(9), 4635–4646. doi: 10.1039/d1ee00627d

Herrera-León, S., Cruz, C., Negrete, M., Chacana, J., Cisternas, L. A., & Kraslawski, A. (2022). Impact of seawater desalination and wastewater treatment on water stress levels and greenhouse gas emissions: The case of Chile. *Science of The Total Environment*, *818*, 151853. doi: 10.1016/j.scitotenv.2021.151853

Hofste, R. W., Reig, P., & Schleifer, L. (2019, 08). *17 Countries, Home to One-Quarter of the World's Population, Face Extremely High Water Stress.* Retrieved from https://www.wri.org/insights/17-countries-home-one-quarter-worlds-population-face-extremely-high-water-stress (Accessed 3 May 2022)

Hurtubia, B., & Sauma, E. (2021). Economic and environmental analysis of hydrogen production when complementing renewable energy generation with grid electricity. *Applied Energy*, *304*, 117739. doi: 10.1016/j.apenergy.2021.117739

IEA. (2018). *Energy Policies Beyond IEA Countries: Chile 2018 Review*. Retrieved from https://www.iea.org/reports/energy-policies-beyond-iea-countries-chile-2018-review

IEA. (2019). *The Future of Hydrogen: Seizing today's opportunities*. Retrieved from https://www.iea.org/reports/the-future-of-hydrogen

IEA. (2020). *Energy Technology Perspectives 2020*. Retrieved from https://www.iea.org/reports/energy-technology-perspectives-2020

IEA. (2021a). *Achieving Net Zero Electricity Sectors in G7 Members*. Retrieved from https://www.iea.org/reports/achieving-net-zero-electricity-sectors-in-g7-members

IEA. (2021b). *Global Hydrogen Review 2021*. Retrieved from https://www.iea.org/reports/global-hydrogen-review-2021

IEA. (2021c). *Hydrogen in Latin America: From near-term opportunities to large-scale*

deployment. Retrieved from https://www.iea.org/reports/hydrogen-in-latin-america

IEA. (2021d). *Net Zero by 2050: A Roadmap for the Global Energy Sector*. Retrieved from https://www.iea.org/reports/net-zero-by-2050

IEA. (2021e). *World Energy Outlook 2021*. Retrieved from https://www.iea.org/reports/world-energy-outlook-2021

IRENA. (2017). *Turning to renewables: Climate-safe energy solutions*. Retrieved from https://irena.org/publications/2017/Nov/Turning-to-renewables-Climate-safe-energy-solutions

IRENA. (2021a). *Decarbonising end-use sectors: Practical insights on green hydrogen*. Retrieved from https://www.irena.org/publications/2021/May/Decarbonising-end-use-sectors-green-hydrogen

IRENA. (2021b). *Sector Coupling in Facilitating Integration of Variable Renewable Energy in Cities*. Retrieved from https://www.irena.org/publications/2021/Oct/Sector-Coupling-in-Cities

Jens, J., Wang, A., van der Leun, K., Peters, D., & Buseman, M. (2021). *Extending the Hydrogen European Backbone: A European hydrogen infrastructure vision covering 21 countries.* Retrieved from https://gasforclimate2050.eu/sdm_downloads/european-hydrogen-backbone/

Li, L., Manier, H., & Manier, M.-A. (2019). Hydrogen supply chain network design: An optimization-oriented review. *Renewable and Sustainable Energy Reviews*, *103*, 342–360. doi: 10.1016/j.rser.2018.12.060

Lorca, A., Sauma, E., & Tapia, T. (2020). *Informe Proyecto ARClim: Sistema Eléctrico.* Centro Energía UC y Centro de Cambio Global UC coordinado por Centro de Ciencia del Clima y la Resiliencia y Centro de Cambio Global UC para el Ministerio del

Medio Ambiente a través de La Deutsche Gesellschaft für Internationale Zusammenarbeit (GIZ). Retrieved from https://arclim.mma.gob.cl/media/informes_consolidados/08_SISTEMA_ELECTRICO.pdf

Mena, R., Escobar, R., Lorca, A., Negrete-Pincetic, M., & Olivares, D. (2019). The impact of concentrated solar power in electric power systems: A Chilean case study. *Applied Energy*, *235*, 258–283. doi: 10.1016/j.apenergy.2018.10.088

Miller, S., Shemer, H., & Semiat, R. (2015). Energy and environmental issues in desalination. *Desalination*, *366*, 2–8. doi: 10.1016/j.desal.2014.11.034

Ministerio de Energía. (2020a). *Carbono neutralidad en el sector energía: Proyección de consumo energético nacional 2020*. Retrieved from https://energia.gob.cl/sites/default/files/pagina-basica/informe_resumen_cn_2019_v07.pdf

Ministerio de Energía. (2020b). *National Green Hydrogen Strategy*. Retrieved from https://www.energia.gob.cl/h2

Ministerio de Energía. (2020c). *Plan de Retiro y/o Reconversión de Unidades de Carbón*. Deutsche Gesellschaft für Internationale Zusammenarbeit (GIZ) GmbH. Retrieved from https://energia.gob.cl/sites/default/files/plan_de_retiro_y_o_reconversion_centrales_carbon.pdf

Ministerio de Energía. (2020d). *Repositorio - Proceso de Planificación Energética de Largo Plazo*. https://energia.gob.cl/pelp/repositorio. Ministerio de Energía. (Accessed 10 October 2021)

Ministerio de Energía. (2021). *INFORME PRELIMINAR Proceso Quinquenal PELP 2023-2027*. Retrieved from https://energia.gob.cl/sites/default/files/documentos/pelp2023-2027_informe_preliminar.pdf

Ministerio de Medio Ambiente. (2020). *4to Informe Bienal de Actualización de Chile*

sobre Cambio Climático.

Muñoz, F. D., Suazo-Martínez, C., Pereira, E., & Moreno, R. (2021). Electricity market design for low-carbon and flexible systems: Room for improvement in Chile. *Energy Policy*, *148*, 111997. doi: 10.1016/j.enpol.2020.111997

Odell, S. D. (2021). Desalination in Chile's mining regions: Global drivers and local impacts of a technological fix to hydrosocial conflict. *Journal of Cleaner Production*, *323*, 129104. doi: 10.1016/j.jclepro.2021.129104

Osorio-Aravena, J. C., Aghahosseini, A., Bogdanov, D., Caldera, U., Ghorbani, N., Mensah, T. N. O., ... Breyer, C. (2021). The impact of renewable energy and sector coupling on the pathway towards a sustainable energy system in Chile. *Renewable and Sustainable Energy Reviews*, *151*, 111557. doi: 10.1016/j.rser.2021.111557

Osorio Aravena, J. C., Aghahosseini, A., Bogdanov, D., Caldera, U., Muñoz-Cerón, E., & Breyer, C. (2020). The role of solar PV, wind energy, and storage technologies in the transition toward a fully sustainable energy system in Chile by 2050 across power, heat, transport and desalination sectors. *International Journal of Sustainable Energy Planning and Management*, *25*, 77–94. doi: 10.5278/ijsepm.3385

Pistocchi, A., Bleninger, T., Breyer, C., Caldera, U., Dorati, C., Ganora, D., ... Zaragoza, G. (2020). Can seawater desalination be a win-win fix to our water cycle? *Water Research*, *182*, 115906. doi: 10.1016/j.watres.2020.115906

Prensa Presidencia. (2019, 06). *Presidente Piñera potencia anuncio de carbono neutralidad al 2050 con líderes de Alemania, Francia, España, Reino Unido y Holanda.* Author. Retrieved from `https://prensa.presidencia.cl/fotonoticia.aspx?id=98046` (Accessed 5 November 2021)

Quiroga, D., Sauma, E., & Pozo, D. (2019). Power system expansion planning under global and local emission mitigation policies. *Applied Energy*, *239*, 1250–1264. doi:

10.1016/j.apenergy.2019.02.001

Reuß, M., Grube, T., Robinius, M., Preuster, P., Wasserscheid, P., & Stolten, D. (2017). Seasonal storage and alternative carriers: A flexible hydrogen supply chain model. *Applied Energy*, *200*, 290–302. doi: 10.1016/j.apenergy.2017.05.050

Samsatli, S., & Samsatli, N. J. (2018). A multi-objective MILP model for the design and operation of future integrated multi-vector energy networks capturing detailed spatio-temporal dependencies. *Applied Energy*, *220*, 893–920. doi: 10.1016/j.apenergy.2017.09.055

Samsatli, S., Staffell, I., & Samsatli, N. J. (2016). Optimal design and operation of integrated wind-hydrogen-electricity networks for decarbonising the domestic transport sector in Great Britain. *International Journal of Hydrogen Energy*, *41*(1), 447–475. doi: 10.1016/j.ijhydene.2015.10.032

Stöckl, F., Schill, W.-P., & Zerrahn, A. (2021). Optimal supply chains and power sector benefits of green hydrogen. *Scientific Reports*, *11*(1), 1–14. doi: 10.1038/s41598-021-92511-6

United Nations Framework Convention on Climate Change. (n.d.). *The Paris Agreement.* Author. Retrieved from `https://unfccc.int/process-and-meetings/the-paris-agreement/the-paris-agreement` (Accessed 3 November 2021)

Verástegui, F., Lorca, A., Negrete-Pincetic, M., & Olivares, D. (2020). Firewood heat electrification impacts in the Chilean power system. *Energy Policy*, *144*, 111702. doi: 10.1016/j.enpol.2020.111702

vom Scheidt, F., Qu, J., Staudt, P., Mallapragada, D. S., & Weinhardt, C. (2022). Integrating hydrogen in single-price electricity systems: The effects of spatial economic signals. *Energy Policy*, *161*, 112727. doi: 10.1016/j.enpol.2021.112727

Vásquez, R., Salinas, F., & Deutsche Gesellschaft für Internationale Zusammenarbeit (GIZ) GmbH. (2019). *Tecnologías del hidrógeno y perspectivas para Chile* (2nd ed.). Deutsche Gesellschaft für Internationale Zusammenarbeit (GIZ) GmbH. Retrieved from https://www.4echile.cl/publicaciones/tecnologias-del-hidrogeno-y-perspectivas-para-chile-2019/

Welder, L., Ryberg, D., Kotzur, L., Grube, T., Robinius, M., & Stolten, D. (2018). Spatio-temporal optimization of a future energy system for power-to-hydrogen applications in Germany. *Energy*, *158*, 1130–1149. doi: 10.1016/j.energy.2018.05.059

Welder, L., Stenzel, P., Ebersbach, N., Markewitz, P., Robinius, M., Emonts, B., & Stolten, D. (2019). Design and evaluation of hydrogen electricity reconversion pathways in national energy systems using spatially and temporally resolved energy system optimization. *International Journal of Hydrogen Energy*, *44*(19), 9594–9607. doi: 10.1016/j.ijhydene.2018.11.194

Yang, G., Jiang, Y., & You, S. (2020). Planning and operation of a hydrogen supply chain network based on the off-grid wind-hydrogen coupling system. *International Journal of Hydrogen Energy*, *45*(41), 20721–20739. doi: 10.1016/j.ijhydene.2020.05.207

APPENDIX

A. NOMENCLATURE OF THE MODEL

The sets presented in the model are described below:

$\mathcal{E} = \{E, H_2\}$	Energy vector (electricity or hydrogen)
$\mathcal{D}$	Representative days (12 days per year, 9 time segments each)
$\mathcal{D}_r$	Time segments specific to representative day r
$\mathcal{G}$	Generation units of the system
$\mathcal{G}^{BES}$	Electric battery units
$\mathcal{G}^{CSP}$	Concentrated solar power plants
$\mathcal{G}^{e}$	Generation units of type e
$\mathcal{G}^{ES}$	All storage units (electricity and hydrogen)
$\mathcal{G}^{H_2S}$	Hydrogen storage units
$\mathcal{G}^{H_2toP}$	Hydrogen-to-power units
$\mathcal{G}^{NonRE}$	Non-renewable generators
$\mathcal{G}^{PV,wind\&hydro}$	Solar PV, wind and hydroelectric generators
$\mathcal{G}^{VRE}$	Variable renewable generators (solar PV, wind power)
$\mathcal{G}_{cand}$	Candidate production units
$\mathcal{G}^{E}_{disp}$	Dispatchable power generators
$\mathcal{G}_{ex}$	Existing production units (as of 2020)
$\mathcal{G}_{n}$	Generation units located at node n
$\mathcal{G}^{e}_{n}$	Generation units of type e located at node n
$\mathcal{G}_{plan}$	Planned production units
$\mathcal{G}_{z}$	Generation units in zone z
$\mathcal{L}$	Lines of the system
$\mathcal{L}^{e}$	Lines of the system for energy vector e

$\mathcal{L}^{e}_{cand}$	Candidate lines for energy vector e
$\mathcal{L}^{e}_{ex}$	Existing lines (as of 2020) for energy vector e
$\mathcal{L}^{e,in}_{n}$	Lines with destination node n for energy vector e
$\mathcal{L}^{e,out}_{n}$	Lines with origin node n for energy vector e
$\mathcal{L}^{e}_{plan}$	Planned lines for energy vector e
$\mathcal{N}$	Nodes (buses) of the system
$\mathcal{N}^{export}$	Hydrogen export nodes
$\mathcal{N}_{z}$	Nodes in zone z
$\mathcal{T}$	Time segments per year (108 time segments)
$\mathcal{Y}$	Target years = {2020,2030,2040,2050}
$\mathcal{Y}^{I}$	Intermediate years before the next target year {0,1,...,9}
$\mathcal{Z}$	Zones of the system

The parameters presented in the model are described below:

γ_1	Reserve share of variable renewable electricity
γ_2	Reserve share of power demand
γ_g	Storage capacity in hours of storage project g
$\Delta_{t,t-1}$	Hours elapsed between time segments $t-1$ and t
Δt_g^{TES}	Hours of storage capacity of CSP unit g
$\delta_{g/ly}$	Binary parameter that indicates whether unit g or line l is available in year y
η_g	Capacity factor of generator g
η_g^C	Efficiency associated with the charging process in storage project g
$\eta_g^{CO_2}$	Emissions production factor (tCO_2/MWh) of power plant g
η_g^{ES}	Round-trip efficiency of storage project g
η_g^{PB}	Electric generator efficiency of CSP unit g
$\eta_g^{\text{SF/TES-PB}}$	PB heat exchange efficiency of CSP unit g
$\eta_g^{\text{SF-TES}}$	TES charging efficiency of CSP unit g
η_g^{TES}	Storing efficiency of CSP unit g
$\eta_g^{\text{TES-PB}}$	TES discharging efficiency of CSP unit g
η_{gt}	Renewable generation profile factor of generator g in time segment t
$\eta_l^{e,L}$	Line losses of line l for energy vector e
λ^{comp}	Electricity consumption for hydrogen compression (MWh/tH_2)
$\lambda_g^{H_2toP}$	Hydrogen consumption for electricity generation (tH_2/MWh)
λ_y^{prod}	Electricity consumption in year y per unit of hydrogen compressed
ω_t	Hours in the year represented by the time segment t
$c_{es}^{ES,fix}$	Annual fixed cost of storage unit g
$c_{es,y}^{ES,inv}$	Annualized investment cost of storage unit g in year y

$c_g^{G,fix}$	Annual fixed cost of generation unit g
c_g^{vom}	Variable operational and maintenance cost of generation unit g
c_{gy}^{fuel}	Fuel price for generation unit g in year y
$c_{gy}^{G,inv}$	Annualized investment cost of generation unit g in year y
$c_l^{L,fix}$	Annual fixed cost of line l
$c_{ly}^{L,inv}$	Annualized investment cost of line l in year y
$c_y^{CO2_2tax}$	Carbon tax price in year y
cap_y	Emissions cap in year y
$d_{H_2,y}^{export}$	Total systemic hydrogen exports demand in year y
$d_{nty}^{e,base}$	Base (exogenous) demand of node n in time segment t for energy vector e
d_{ye}^{rate}	Discount factor of year ye referenced to 2020
$f_l^{\max}$	Energy transport capacity of line l
h_g	Fuel consumption factor of generation unit g
k	Number of years between target years
$\overline{k_{l/g}^{G/L}}$	Maximum investment levels of unit g or line l
$p_g^{\max}$	Generation capacity of existing or planned unit g
q_{gt}^{SF}	Solar field thermal power available for unit g in time t (MWt)

The variables presented in the model are described below:

$B^{ES}_{es,y}$	Capacity addition to storage unit es in year y
$B^{G/L}_{g/ly}$	Capacity addition to unit g or line l in year y
C^{T}_{y}	Total systemic costs in year y
$C^{T'}_{y+y^I}$	Interpolated total cost in year y^I after year y
$D^{e_2}_{e_1,nty}$	Demand of vector e_1 to produce vector e_2 in node n, time segment t and year y
E^{ES}_{gty}	Stored energy in storage unit g in time segment t in year y
E^{TES}_{gty}	Stored thermal energy in TES CSP unit g in time segment t in year y (MWh_t)
F_{lty}	Line flow (MW or tonH_2/hr) of line l in time segment t in year y
FixedCosts_y	Systemic fixed costs in year y
InvCosts_y	Systemic annualized investment costs in year y
$K^{ES}_{es,y}$	Cumulative installed capacity of storage unit es in year y
$K^{G/L}_{g/ly}$	Cumulative installed capacity of unit g or line l in year y
P_{gty}	Production (MW or tonH_2/hr) of asset g in time segment t in year y
Q^{EX}_{gty}	Excess thermal power of CSP unit g in time segment t in year y (MW_t)
$Q^{e,C}_{gty}$	Charge flow of storage unit g of vector e in time segment t in year y
$Q^{e,D}_{gty}$	Discharge flow of storage unit g of vector e in time segment t in year y
$Q^{TES,C}_{gty}$	Charge thermal flow of CSP unit g in time segment t in year y (MWh_t)
$Q^{TES,D}_{gty}$	Discharge thermal flow of CSP unit g in time segment t in year y (MWh_t)
VarOpCosts_y	Systemic variable operational costs in year y

B. DERIVATION OF 2050 MARGINAL COST SCALING FACTOR

Due to the structure of the objective function, that includes both a discounting factor and linear interpolations between consecutive target years, a scaling factor requires to be calculated to estimate the total marginal costs for electricity (or hydrogen) supply. We begin by thoroughly explaining the method to obtain the 2050 scaling factor and then derive the factors for the rest of the target years included in this study. First, we define Δ_{2050} as the change caused in the objective function due to a marginal increase in the electricity (or hydrogen) balance constraint in 2050, which can be obtained from the dual variables of these constraints from the model's solution. We then define MC_{2050} as the total marginal cost (in 2050's prices), and similarly, C_{2050} as the total cost in 2050. Thus, we are interested in calculating the scaling factor ϵ_{2050} as follows:

$$\Delta_{2050} = \epsilon_{2050} \cdot MC_{2050} \tag{B.1}$$

Given the structure of the objective function, a marginal increase in the energy balance constraint only affects consecutive target years. In this case, a marginal change in 2050 would only affect from 2041 onwards (2050 is the final year analyzed). The objective function, considering only the cost variables from 2040 onwards, can be written as follows:

$$OF = d_{20}^{factor} C_{2040} + d_{21}^{factor}[C_{2040} + (C_{2050} - C_{2040}) \cdot \frac{1}{10}] + d_{22}^{factor}[C_{2040} + (C_{2050} - C_{2040}) \cdot \frac{2}{10}] + ... + d_{30}^{factor} C_{2050} \tag{B.2}$$

We remind that d_i^{factor} refers to the discount factor of year i relative to 2020. Now, when calculating the marginal change in the objective function due to a marginal increase in the energy supply balance in 2050, we can directly estimate the scaling factor as follows:

$$\Delta_{2050} = d_{20+i}^{factor} \sum_{i=1..10} \frac{i}{10} MC_{2050} = \epsilon_{2050} \cdot MC_{2050} \tag{B.3}$$

Similarly, we derive the scaling factors for 2020, 2030 and 2040:

$$\Delta_{2020} = d_{i}^{factor} \sum_{i=0..9} (1 - \frac{i}{10}) MC_{2020} = \epsilon_{2020} \cdot MC_{2020} \tag{B.4}$$

$$\Delta_{2030} = [d_{i}^{factor} \sum_{i=1..10} \frac{i}{10} + d_{10+i}^{factor} \sum_{i=1..9} (1 - \frac{i}{10})] MC_{2030} = \epsilon_{2030} \cdot MC_{2030} \tag{B.5}$$

$$\Delta_{2040} = [d_{10+i}^{factor} \sum_{i=1..10} \frac{i}{10} + d_{20+i}^{factor} \sum_{i=1..9} (1 - \frac{i}{10})] MC_{2040} = \epsilon_{2040} \cdot MC_{2040} \tag{B.6}$$

C. OTHER CASE STUDY INPUTS

Table C.1. Node numbering.

Node number	Node name
1	Parinacota220
2	NuevaPozoAlmonte220
3	Lagunas220
4	Kimal220
5	Kimal500
6	LosChangos220
7	LosChangos500
8	NuevaZaldivar220
9	Parinas500
10	Cumbre500
11	NuevaCardones500
12	NuevaMaitencillo500
13	NuevaPandeAzucar500
14	Quillota500
15	Polpaico500
16	AltoJahuel500
17	Candelaria500
18	Rapel500
19	Ancoa500
20	Concepcion500
21	NuevaCharrua500
22	Mulchen500
23	RioMalleco500
24	Pichirropulli500
25	NuevaPuertoMontt500
26	NuevaAncud500

Source: Own elaboration based on Ministerio de Energía (2020d).

Table C.2. Nodal grouping by zone.

Zone	Nodes included
North	1-13
Center	14-18
South	19-26

Source: Own elaboration based on Ministerio de Energía (2020d).

Table C.3. Number of existing power generation units by technology and system zone in the case study data.

Technology/Zone	North	Center	South	**Total**
Biogas	0	6	3	**9**
Biomass	0	3	17	**20**
Coal	21	4	4	**29**
Cogeneration	1	2	2	**5**
CSP	1	0	0	**1**
Diesel	30	28	47	**105**
Electric battery	0	0	0	**0**
Gas	7	10	4	**21**
Geothermal	1	0	0	**1**
H_2CCGT	0	0	0	**0**
Hydro Dam	0	1	9	**10**
Hydro Run of River	9	36	99	**144**
Solar PV	66	105	20	**191**
Wind	17	1	15	**33**
Total	**153**	**196**	**220**	**569**

Source: Adapted from Ministerio de Energía (2020d).

Table C.4. Number of planned and candidate power generation units by technology and system zone in the case study data.

Technology/Zone	North	Center	South	**Total**
Biogas	0	0	0	**0**
Biomass	0	0	6	**6**
Coal	0	0	0	**0**
Cogeneration	0	0	0	**0**
CSP	124	0	0	**124**
Diesel	8	0	5	**13**
Electric battery	13	5	8	**26**
Gas	22	0	7	**29**
Geothermal	7	1	4	**12**
H_2CCGT	13	5	8	**26**
Hydro Dam	0	0	0	**0**
Hydro Run of River	0	8	72	**80**
Solar PV	101	43	26	**170**
Wind	37	3	77	**117**
Total	**325**	**65**	**213**	**603**

Source: Adapted from Ministerio de Energía (2020d).